gear TECHNOLOGY®

MAY 2022

SURFACE FINISHING

- HOBBING AND CHAMFER CUTTING
- GRINDING
- NANOFLUIDS FOR PRODUCTION GAINS

www.geartechnology.com

Gear Technology is published by **The American Gear Manufacturers Association**


FFG
EUROPE
MODUL
CDA 250

gear TECHNOLOGY®

MAY 2022

A Publication of
The American Gear Manufacturers Association

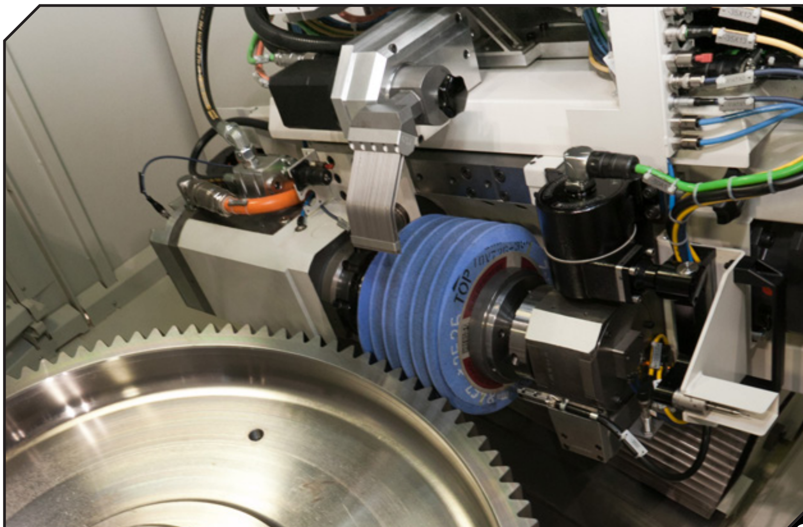

30

features

technical

Stay Connected

Join the Gear Technology Facebook group at
www.facebook.com/help/312721188838183

Connect with us on LinkedIn
www.linkedin.com/groups/3893880/

Follow us on Twitter
twitter.com/Gear_Technology

Subscribe Online
www.geartechnology.com/subscribe.htm

Vol. 39. No. 1 GEAR TECHNOLOGY. The Journal of Gear Manufacturing (ISSN 0743-6858) is published monthly, except in February, April, October and December by The American Gear Manufacturers Association, 1840 Jarvis Avenue, Elk Grove Village, IL 60007, (847) 437-6604. Cover price $7.00 U.S. Periodical postage paid at Arlington Heights, IL, and at additional mailing office (USPS No. 749-290). The American Gear Manufacturers Association makes every effort to ensure that the processes described in GEAR TECHNOLOGY conform to sound engineering practice. Neither the authors nor the publisher can be held responsible for injuries sustained while following the procedures described. Postmaster: Send address changes to GEAR TECHNOLOGY. The Journal of Gear Manufacturing. 1840 Jarvis Avenue, Elk Grove Village, IL, 60007. Canadian Agreement No. 40038760.

gear TECHNOLOGY®

Vol. 39. No. 1

departments

THE GEAR INDUSTRY'S INFORMATION SOURCE

www.geartechnology.com

GT Revolutions

Liebherr Helps Customers Master E-Mobility Gear Challenges

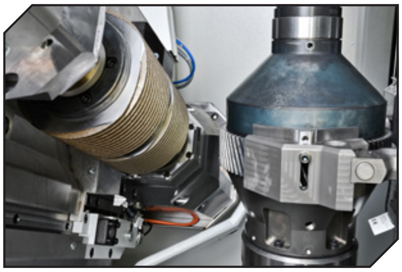

New drive technologies in e-mobility are changing the requirements for gears and, therefore, the quality of the tooth-flank surfaces. Manufacturers of gears have to adapt their manufacturing process accordingly.

geartechnology.com/blogs/4-revolutions/post/29840-liebherr-helps-customers-master-e-mobility-gear-challenges

Process Variables for Gear Grinding

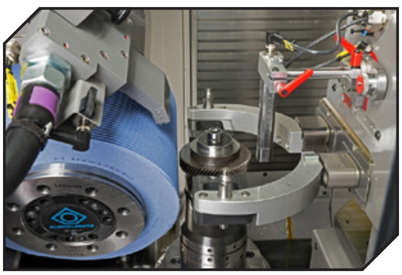

Tremec's dual-clutch transmission development utilizes Klingelnberg's Speed Viper gear grinding technology. The two companies have collaborated on projects since 1993. This case study examines the advantages of closed-loop technology.

geartechnology.com/blogs/4-revolutions/post/29827-process-variables-for-gear-grinding

Gleason Profile Grinding

Grind internal and external gears up to 800 mm in diameter with Gleason´s P600/800G Profile Grinding Machine including on-board gear inspection. Adaptable to many different gear applications with different grinding heads for a variety of wheel diameters as well as internal grinding head with different grinding arms.

geartechnology.com/media/videos/play/237-gleason-profile-gear-grinding

gear TECHNOLOGY®

AGMA MEDIA
1840 JARVIS AVENUE
ELK GROVE VILLAGE, IL 60007
(847) 437-6604
FAX: (847) 437-6618

EDITORIAL

Publisher & Editor-in-Chief
Randy Stott, Vice President Media
stott@agma.org

Senior Editor
Matthew Jaster
jaster@agma.org

Senior Editor
Aaron Fagan
fagan@agma.org

Technical Editors
William (Bill) Bradley, Robert Errichello, John Lange, Joseph Mihelick, Charles D. Schultz, P.E., Robert E. Smith, Mike Tennutti, Frank Uherek

DESIGN

Art Director
David Ropinski
ropinski@agma.org

ADVERTISING

Associate Publisher & Advertising Sales Manager
Dave Friedman
friedman@agma.org

Materials Coordinator
Dorothy Fiandaca
fiandaca@agma.org

CIRCULATION

Circulation Manager
Carol Tratar
tratar@agma.org

ACCOUNTING

Accounting
Luann Harrold
harrold@agma.org

MANAGEMENT

President
Matthew E. Croson
croson@agma.org

FOUNDER

Michael Goldstein founded Gear Technology in 1984 and served as Publisher and Editor-in-Chief from 1984 through 2019. Thanks to his efforts, the Michael Goldstein Gear Technology Library, the largest collection of gear knowledge available anywhere, will remain a free and open resource for the gear industry. More than 36 years' worth of technical articles can be found online at *www.geartechnology.com*. Michael continues working with the magazine in a consulting role and can be reached via e-mail at *michael@geartechnology.com*.

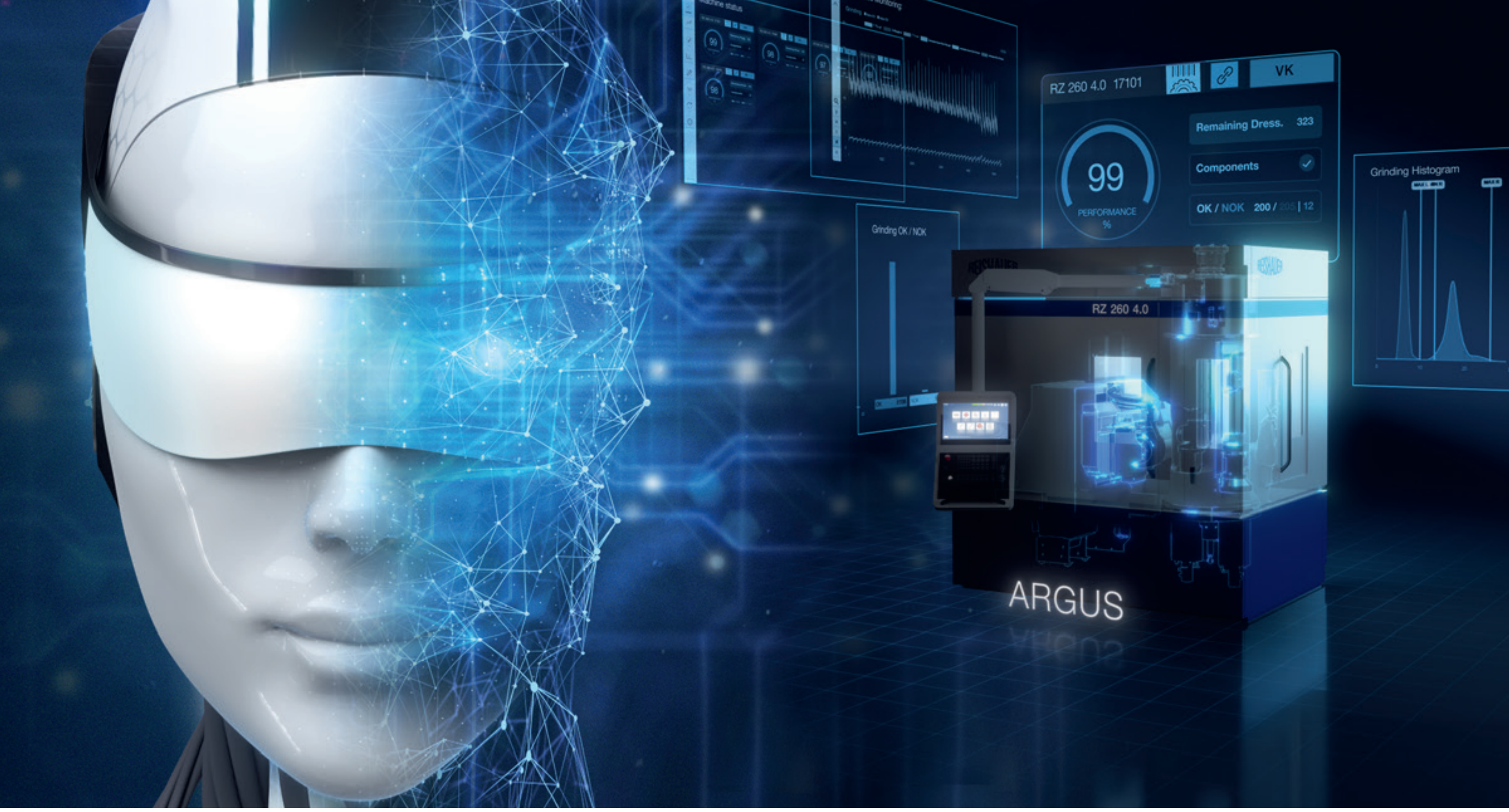
RZ 260 4.0 17101
VK
Remaining Dress. 323
Components
99
PERFORMANCE
%
Grinding Histogram
Grinding OK / NOK
RZ 260 4.0
ARGUS

Up Close and Personal

Publisher & Editor-in-Chief
Randy Stott

After more than two years of COVID isolation, it feels good to be getting out of our bunkers and interacting with people again.

Last month, I had the great pleasure of attending the AGMA Annual Meeting, where executives from member companies got together in person for the first time since 2019. The 2020 meeting was canceled at the last minute due to COVID. Last year's meeting was held virtually, with an electronic meeting room and videoconference presentations. But this year felt like a return to normal.

Held at the PGA National Resort and Spa in Palm Beach Gardens, Fla., the event attracted well over 200 participants, including gear manufacturers, industry suppliers and guests. Although this wasn't a record crowd, it was a healthy one, and there was plenty of networking, learning and collaboration going on. But more importantly, there was laughter, there was camaraderie and there was fun. In fact, this reporter observed quite a few of our advertisers, authors and long-time readers cutting loose on the dance floor (names are being withheld to protect the innocent).

It was good to see the gear industry come together in that way.

But the event was more than just fun and games. There were a number of presentations on future trends that will impact the industry, including topics like demographics, artificial intelligence, robotics, supply chain and the annual economic forecast by Jim Meil of ACT Research.

A number of deserving gear industry contributors also received awards at the event.

The late Wendy Young, president of Forest City Gear, who passed away in February, posthumously received the AGMA Chairman's award, which is presented to individuals who have:

- Contributed in a meaningful way to the promotion of the gear industry.
- Acted above and beyond the call of duty to support AGMA.
- Acted unselfishly by getting the job done.
- Tirelessly supported and promoted the organization.
- Advanced the goals of AGMA and the gear industry through work done on behalf of the organization.
- Led or supported a major initiative with the organization.

Young's award was accepted by her daughters Mindy, Kika and Appie, with husband Fred Young attending via videochat.

The Chairman's Award was also presented to Cindy Bennett, in recognition of her years of service as the former Director of the AGMA Foundation.

"The AGMA is blessed to have always had outstanding leadership and guidance over its 106 years and the recognition of these industry leaders is no exception," said Matthew Croson, AGMA President. "They all went above and beyond to support growth, foster innovation, and create positive, meaningful connections."

In addition, the association presented its Hall of Fame Award to Martin Kapp of Kapp-Niles. "Martin Kapp is a true hall of famer, blessed with both technical ability and natural charm. He has worked hard to build a company that supports AGMA members' innovation efforts, while maintaining a strong character—everyone recognizes Martin's humble nature," Croson said. "We wish Martin the very best as he enjoys his well-deserved retirement, while continuing to develop the next generation of Kapp leadership."

Most everyone I talked to indicated to me that the annual meeting was a great success. Nearly every conversation was filled with enthusiasm and vigor. People are truly happy to be able to get together again. Lifelong friendships get built at meetings like this one, even among competitors. I witnessed the truth of that by seeing the interactions of the participants. And it's not just the old timers, either. There were more than 50 first-time participants at this annual meeting, and I daresay that I also witnessed some lifelong friendships that have just begun.

The NIDEC ZI20A-G Generating Internal Gear Grinder

Nidec Machine Tool America

The world's first and only threaded wheel internal gear grinder. Now available with Siemens CNC.

MSS300 Skiver

GE15HS Hobber

FE30A Shaver

ZE26C Gear Grinder

This issue's focus is internal gear grinding with the **ZI20A-G**: fast, consistent, economical and productive processing of parts up to 200mm ID.

We can help you make quiet internal gears for planetary ***EV transmissions***.

ZI20A-G Internal Gear Grinder

ST40A Shaper

Threaded wheel internal gear grinding using unique multi-start tool. High speed grinding velocity is developed with the crossed axis angle.

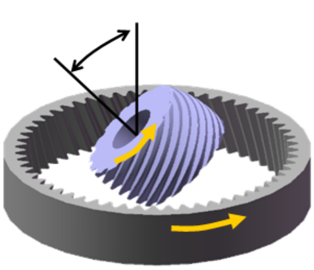

Call now to schedule a test grind of your parts. ***We have you covered!***

Visit **www.nidec-machinetoolamerica.com** and call our sales department at **248-669-6136**

LEGENDARY RELIABILITY

Hobbing and Chamfer Cutting

EFFICIENT, FLEXIBLE GEAR MANUFACTURING ON A SINGLE MACHINE

GOTTFRIED KLEIN, DIRECTOR OF PRODUCT MANAGEMENT
HOBBING, CHAMFERING, AND SHAVING
GLEASON CORPORATION

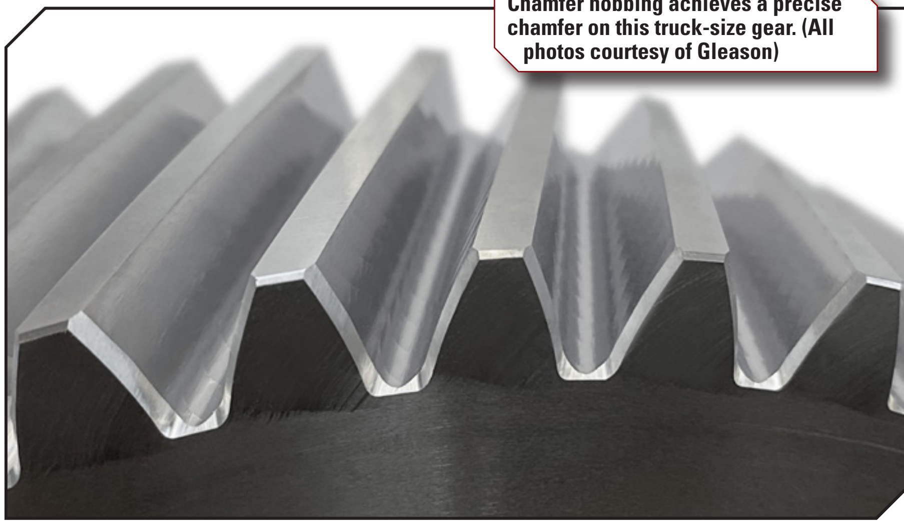

Chamfer hobbing achieves a precise chamfer on this truck-size gear. (All photos courtesy of Gleason)

It wasn't long ago that cylindrical gear chamfering and deburring was almost an afterthought. Now the process ranks as high in importance as hobbing, shaping and grinding. Seemingly every gear manufacturer, particularly those developing transmission gears for e-drive applications, recognizes that anything less than a flawless tooth flank can result in premature transmission failure, less-than-optimal efficiency, and unacceptable noise. Thus, generating a chamfer to precise customer specifications is critical to minimize the potential for sharp, brittle edges after heat treat; avoid edge load situations in the gearbox; and eliminate excessive stock and hardened burrs in the tooth flank prior to the hard finishing operations (conditions which can greatly diminish tool life).

280HCD—the Single-Machine Solution

For producers of spur and helical gears in sizes up to module 5 mm with 280 mm workpiece outside diameter and 380 mm shaft lengths, two chamfering processes now exist: chamfer hobbing, for high volume automotive and light truck applications, including final drive ring gears and shafts; and fly cutter chamfering, delivering flexibility for lower volume, small lot jobber applications. Chamfer hobbing first became available on Gleason machines with the Genesis 160HCD vertical Hobbing and Chamfering Machine, then the range was expanded to include even truck-size gears with introduction of the Genesis 280HCD. Fly cutter chamfering, which had long been employed on bevel gear cutting machines, was adapted for the first time as a viable chamfering process for cylindrical gears on Gleason's Genesis 400HCD Hobbing Machine, designed for workpieces up to 450 mm outside diameter and module 8 mm. Yet, for many gear manufacturers, it's not an either-or proposition. Most can benefit from a *single* platform that can perform both processes interchangeably, and thus open the door for many new opportunities, whether with an increase in productivity, or through the production of smaller lots requiring tremendous flexibility.

The 280HCD combines hobbing with a chamfering/deburring station attached

280HCD Hobbing and Chamfering machine with chamfer station for chamfer hobbing and fly cutter chamfering.

to perform either chamfer hobbing or fly cutter chamfering in parallel to the hobbing operation. The 280HCD features a gantry loader to link gear hobbing with the chamfer cutting station and external automation/storage. Most importantly, users can benefit from having both chamfering processes on the same machine and at their disposal with just a simple tool change.

Low tool cost per piece

The Gleason Chamfer Hob has characteristics very similar to a conventional gear hob. A Chamfer Hob is used for each tooth flank with a tooth profile specifically designed for the particular chamfer form that is required. This design delivers great flexibility: comma or parallel-chamfer forms are possible, as well as chamfers along the tooth edge only or including the root area. By cutting into the gap, burrs are avoided on the face side of the gears; no measurable burrs on the flank are produced, and downstream processes to remove the burr are eliminated. Finally, the Gleason Chamfer Hobbing process offers tool shifting, which delivers increased tool life resulting in a low tool cost per piece.

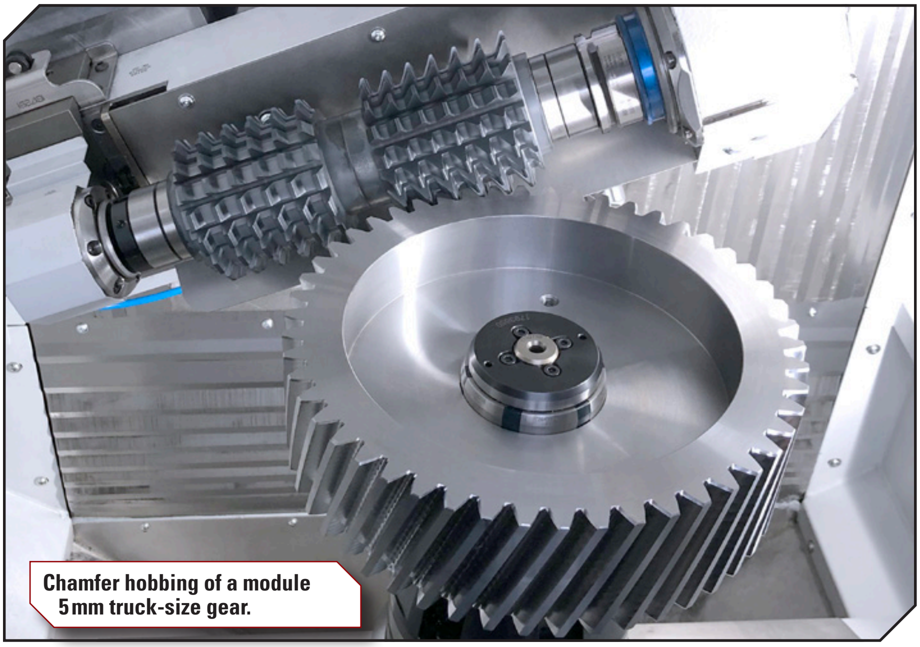

Chamfer hobbing of a module 5 mm truck-size gear.

Flexibility on the fly

Having to employ dedicated chamfering tools for each and every workpiece can be time-consuming and cost prohibitive. Fly cutter chamfering on-board can assist with this. Chamfer size and angle can easily be entered into the machine's intuitive *GEMS* operator interface. The process generates a chamfer along the gear edge contour by synchronizing a fly cutter with workpiece rotation such that the fly cutter—generally a star-shaped body with two to four standard indexable carbide inserts—mills the chamfer with the desired characteristics. Since each edge of the tooth is done separately and the chamfer size and angle depend on machine movements and not on the tool design, the process is quite universal. With just a relatively few different standard (i.e., inexpensive and globally available) insert blade sets and base cutter bodies, a single tool can be used for different modules, pressure angles, and numbers of teeth.

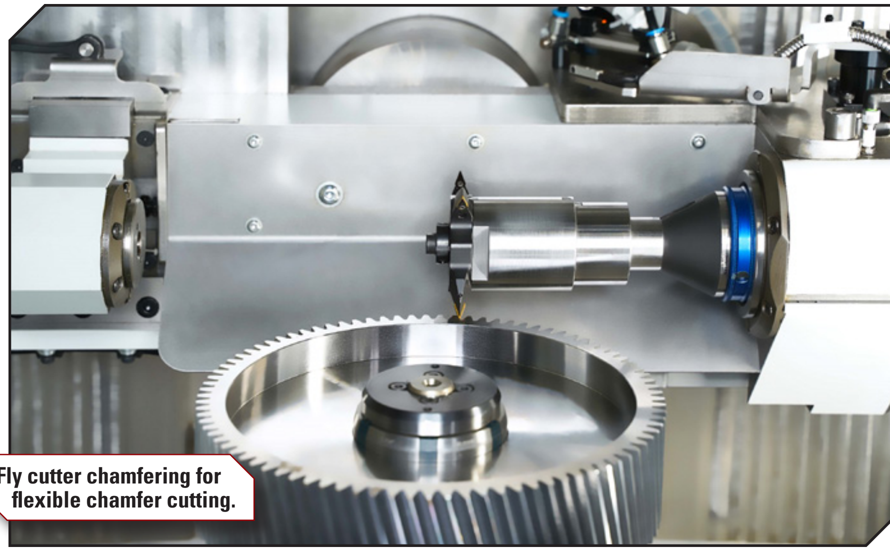

Fly cutter chamfering for flexible chamfer cutting.

Introducing 280CD: Standalone Chamfering

The new 280CD Gear Chamfering Machine, essentially the chamfering station of the 280HCD, can operate as a stand-alone machine to service one, or multiple, hobbing machines, or be fully integrated by Gleason Automation Systems' robotics solution to existing machines. Spur and helical gears in the size range produced by the 280CHD Hobbing Machine and described previously, can be accommodated. (*Editor's Note: Gleason will exhibit the 280CD at both the upcoming IMTS and AMB shows.*)

280HCD—The Complete Machine

The gear-driven hob head, delivering speeds up to 2,000 rpm, combined with several hob clamping alternatives, ensures every application can benefit from the best possible cutting tool solutions, now and in the future. For dry cutting, for example, the latest G50, G90, or carbide hob material is ideal. Several chip evacuation options ensure dry, hot chips won't interfere with the highly productive cutting process. Wet cutting options with magnetic chip conveyor are available as well.

The 280HCD's CNC tailstock will support clamping disc-type workpieces as well as shaft-type parts as long as 380 mm, using the fast, adaptable Quick-Flex Plus workholding system, which cuts workholding changeover in both the hobbing and chamfering workareas to under a minute each.

Like all the latest generation of Gleason machines, the 280HCD is supported by Gleason's complete manufacturing system, including hobs, milling cutters and chamfer hobs, modular workholding and smart grippers, as well as process engineering and ongoing training to help ensure the system is operating at peak efficiencies and producing the optimum in quality.

Shorter cycle times and more efficient, error-free operation also result from Gleason's latest *GEMS Hobbing Operator Interface*, which makes setup and changeover intuitive and simple to learn. The *GEMS Interface*, coupled with Siemens' 840Dsl control, provides several new process options and guides the operator intuitively through the workflows of the machine.

gleason.com

EMAG

SERVES E-MOBILITY NEEDS AT LINAMAR TECHNOLOGY HUNGARY

Linamar Technology Hungary — a specialist for e-drives — recently invested in machines from EMAG for gear and shaft production. The number of components is expected to increase to more than 2,000,000 pieces per year in the future — up from around 300,000 pieces at present. The new production solution is optimally prepared for this increase.

Linamar Technology Hungary uses the EMAG VL 6 and VT 2-4 vertical lathes and the VLC 200 GT vertical turning and grinding center for hard machining of gears and shafts. The company also has the ELC 160 laser welding machine for welding gear wheels. The VLC 200 GT turning and grinding center illustrates EMAG's holistic approach: the machine is loaded at a particularly high speed by the integrated pick-up spindle. After the spindle with the component has assumed its machining position, hard rough turning starts in quick succession. Only a residual allowance of a few micrometers then remains on the gear wheel. This ensures a significantly shortened grinding process with the aid of the integrated grinding spindle.

At the same time, the machining quality benefits from the turning-grinding combination: If only a small allowance needs to be ground off after turning, the grinding wheel specification can be more specifically designed for the desired final quality. Overall, Linamar's production planners can therefore dispense with a further grinding operation.

Linamar has seen similar leaps in productivity with its VL 6 and VT 2-4 lathes, which are used for turning operations on gears and shafts of different sizes. Depending on the size and type of component, the machining task differs. For example, the VT 2-4 automated vertical lathe provides leaps in performance for shaft machining, removing a hardened layer in the weld area. The strength of this system is particularly evident with higher quantities because its automation

solution ensures fast chip-to-chip times: workpiece grippers are used to transport the unmachined parts into the machine and remove them again after machining. Depending on the workpiece, this changeover time takes only six to eight seconds. In high-volume production, these short nonproductive times add up to enormous time savings. The actual turning process also takes place in short cycles: The shaft is clamped vertically between the main spindle and the tailstock and machined from two sides. Two tool turrets with twelve places each are available for this purpose, which can be equipped with turning tools or driven tools.

The Vertical Lathe VL 6 is again used for machining several areas on gears with diameters of over 200 mm. The components are also part of an electric drive system. Their function is to reduce the high speed of the electric motor to the lower level of wheel rotation. The VL 6 used here is being developed by EMAG for larger workpieces, and the machine also has integrated automation. It is equipped with a workpiece storage conveyor and loads/unloads via pick-up spindle.

"We are currently in the start-up phase and produce around 60,000 parts per type per year. In the future, however, we will produce around 430,000 parts per type per year," said István Bíró, project manager at Linamar Technology Hungary. "In this respect, it is important for us that the machines ensure a stable process. This is absolutely the case. In addition, we have not yet completely exhausted the potential of the machines at present. For example, we can reduce the measuring effort if we use the integrated measuring probes. Overall, we are very satisfied with the solution."

emag.com
linamar.com

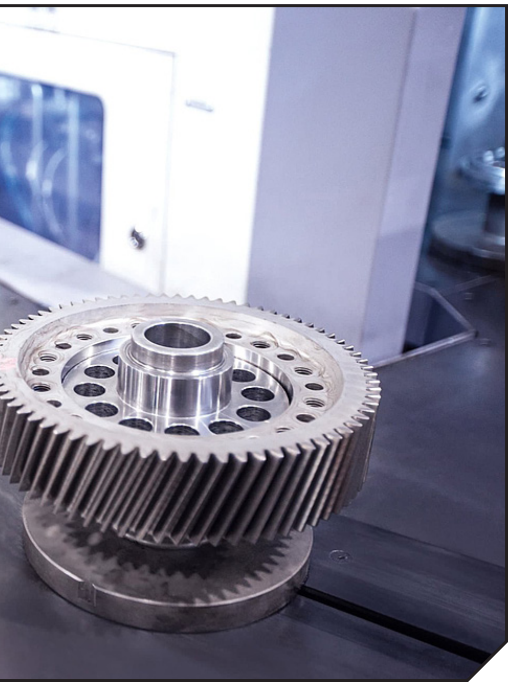

Seco Machine Monitoring

PROVIDES PRODUCTION EFFICIENCY

Manufacturers need to measure and quantify the causes of unproductive time so they can optimize their efficiency. Machine Monitoring from Seco provides them with the data-driven knowledge they need to not only manage production efficiency, but also increase both output volume and product quality.

Done in real time and remotely, Seco Machine Monitoring solutions sample production data on a continuous basis to build a full picture of what happens on a manufacturer's shop floor. These insights build an in-depth profile of daily activity and trigger alerts for onsite response or remote notification of production-critical metrics.

Detailed insights into machining operations on all attended and unattended shifts make it easy for manufacturers to track Overall Equipment Effectiveness (OEE) and make continuous improvements to operations for better planning, scheduling and communication. Overall, such data-driven insights reveal the real root causes of production problems that hinder workflow optimization.

Limited access to real-time production data slows a manufacturer's response to individual applications, machines, cells and overall production workflow. With a low entry cost, Seco Machine Monitoring provides enhanced communication from the shop floor to upper management based on data-driven smart manufacturing.

Color-coded metrics on real-time dashboards give manufacturers the insights they need to improve efficiency. Employees are also able to easily add their insights and observations, categorize machine downtime and help contextualize problems. These best-in-class service solutions come courtesy of partnerships with an exclusive network of state-of-the-art software providers and technology partners like MachineMetrics.

Rather than offer customers data-gathering solutions that merely accrue information from production processes, Seco provides a robust portfolio of solutions. For every challenge that limits manufacturing effectiveness, Seco draws on a continuing stream of unduplicated insights gained through decades of manufacturing expertise to create solutions in partnership with customers.

While data and analytics are valuable to manufacturers, these tools take on even greater importance within the context of a broader set of Seco support options that address everything from employee technical education to tool-use optimization. Such a big-picture emphasis — through a partnership for continuous improvement with the customer — fosters collaboration and a full understanding of machine capacity.

secotools.com

Index

ANNOUNCES NEXT GENERATION TNL12 SLIDING HEADSTOCK CNC LATHE

Index has announced the launch of the next generation of its Traub TNL12 sliding-headstock lathe for small part machining. Representing a comprehensive evolution of the machine, the new TNL12 incorporates a plethora of design changes that boost speed, flexibility and accuracy.

The new machine provides an especially strong value proposition for medical manufacturers responsible for producing implants, bone screws and instruments for minimally invasive surgery.

Like its predecessor, the new TNL12 features four tool carriers that can be applied to a workpiece simultaneously, albeit with significant changes to the machine's kinematics. While the front-working attachment and counter

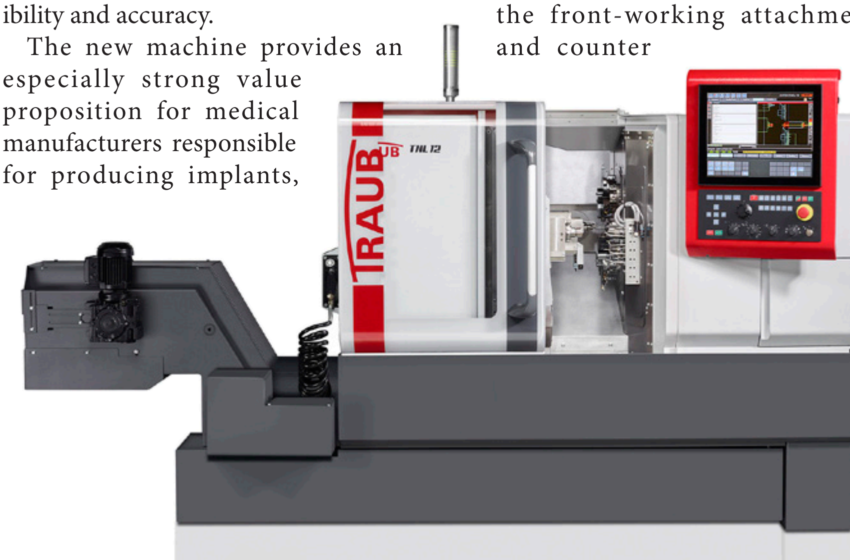

spindle were previously arranged on a single slide, they are now housed on separate slides. This eliminates potential interdependence between front-end and counter spindle machining, allowing for much greater flexibility in programming. Additionally, this design reduces the mass of both elements, allowing for faster and more dynamic machine response.

The features enabling rear-end machining also have undergone substantial changes. While the former model of the machine offered x-axis machining on the counter spindle, the new TNL12 provides full three-axis machining in this position. A new back-working attachment offer six tool stations, with up to four allowing live tooling, as well as a flushing unit.

Overall tooling capacity has also been increased, with the capability to house up to 40 tools with the use of double and triple holders. This allows operators a greater degree of freedom to optimize machining of highly complex parts. Each of two six-station tool turrets has its own servomotor and interpolated y-axis, with chip-to-chip tool change times reduced to just 0.3 seconds.

While the previous generation TNL12 used belt drives on the main and counter spindles, the new machine incorporates fluid-cooled motor spindles with a maximum speed of 12,000 rpm. The new TNL12 also offers higher dynamic response thanks to low-mass clamping cylinders and a carbon sleeve for the guide bushing drive. The guide bushing is freely selectable, live or programmable, with the ability to adjust itself via a pneumatic servo valve.

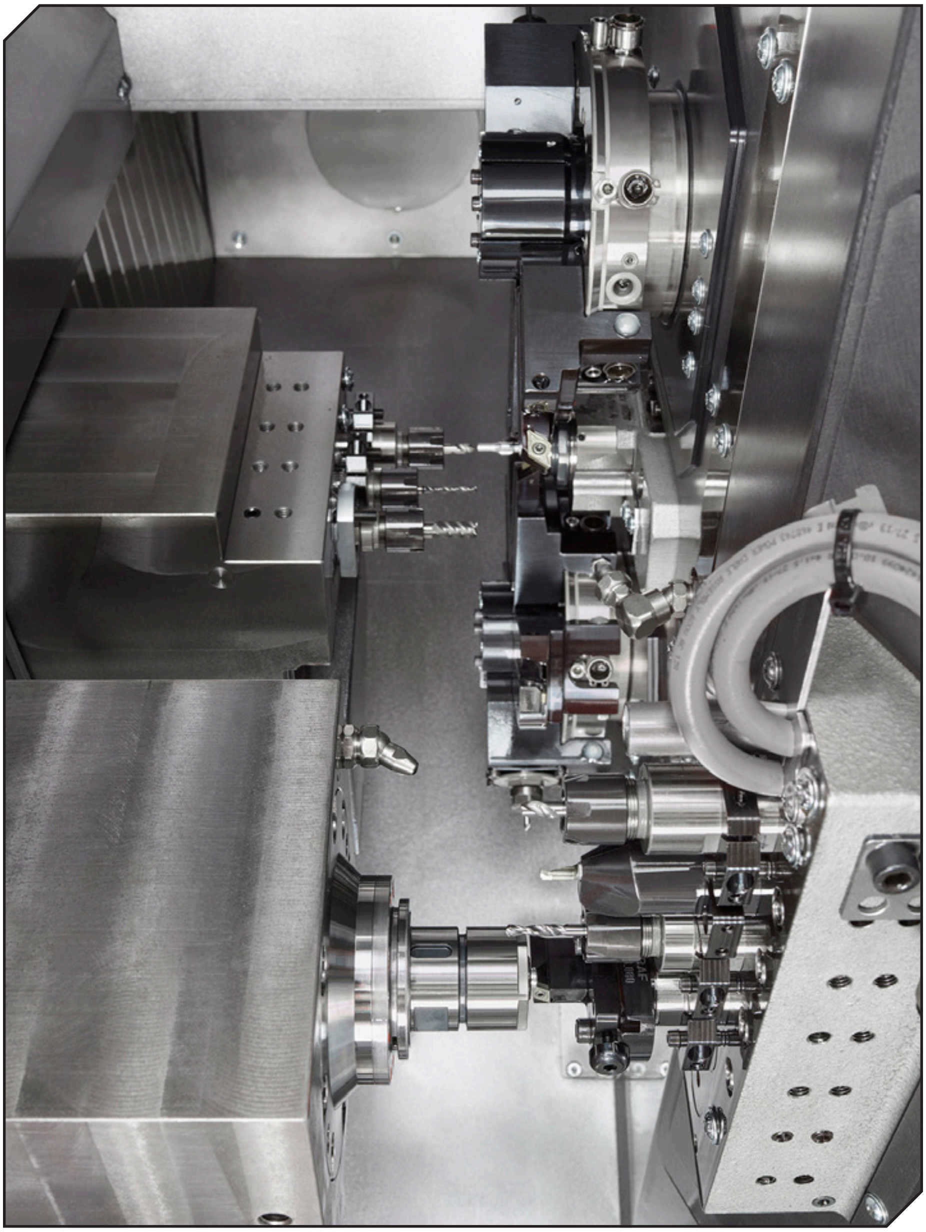

Refinements to the TNL12's overall structure include a non-hydraulic design, gray cast iron bed and thermo-symmetrical design that increases thermal accuracy and reduces warm-up times. These and other features combine to increase the stability of the machine, resulting in even higher accuracy and shorter cycle times.

The new TNL12 includes an eight-bar coolant pump, with the option to add one or two adjustable pumps capable of 20 bar to 120 bar. A 250-bar pump is also available for special applications. Coolant is cleaned by a compact belt filter and users can choose between a tray or conveyor for chip removal.

To maximize the potential for unmanned operation, the TNL12 offers options for automated rinsing, part removal via a small gripper and removal of long parts through the counter spindle. The machine can also be paired with a robot for machining of chucked parts. Furthermore, the machine can be equipped with an optional whirling unit with a +/- 30-degree swivel angle for high-speed whirling to a length of 75 mm.

The new TNL12 incorporates the current Traub TX8i-s control, which offers Industry 4.0 connectivity via Index's *iXworld* platform. The folding and swiveling operating panel include a 19" touchscreen and provides easy access to a networked production environment.

us.index-traub.com/tnl12

Gastops

EXPANDS ENGINE TEST CELL R&D

Gastops is supporting Virtual Vehicle's latest initiative in conducting high-performance engine test cell research and development, supplying custom oil-debris monitoring solutions with MetalSCAN.

MetalSCAN provides customers' operating engine and gearbox test cells with essential conditioning monitoring technology, enabling evaluation, and testing of components and systems to measure real-time equipment health, performance and predict the remaining useful life (RUL) of critical components.

MetalSCAN delivers real-time equipment monitoring by offering a full flow, nonobstructive, online wear-debris detection system. The design features, coupled with the ability for early detection of equipment failure, empower customers to manage and optimize their testing program, conduct root-cause analysis, and minimize costs by limiting damage to critical components.

Says Dr. Hannes Allmaier, Ph.D., Dipl.-Ing. team leader tribology and efficiency group at Virtual Vehicle Research GmbH, "MetalSCAN proves itself to be a vital tool in our engine testing operation by detecting the initial onset and monitoring the progression of component damage. The indications allow us to manage the engine operational characteristics, maximize testing and prevent secondary component damage. With limiting damage, we are able to complete successful root cause analysis investigations."

gastops.com/products-services/metalscan

Southern Gear

EXPANDS BEVEL GEAR PRODUCTION

Southern Gear has added two rebuilt Gleason No. 102 Generators to its production capabilities to meet growing demand for smaller, high-precision straight bevel gears produced with the Coniflex process.

The 102s add capacity to Southern Gear's straight bevel gear production capability, which also includes Gleason No. 14 and No. 104 Coniflex Generators.

"While these dedicated, manually operated machines might seem out of place alongside the advanced CNC machines occupying most of our shop floor, they are still an excellent solution for the production of small straight bevel gears using the highly desirable Coniflex method," explains Southern Gear President Karen Malin. "Most importantly, we have the experience and operators needed to take full advantage of these machines."

The addition of the Gleason 102 Generators is part of a multimillion-dollar, company-wide investment in new technologies, methodologies and processes that, over the last several years, has, according to Malin, added much needed capacity to Southern Gear's vertically integrated shop floor.

southerngear.com

Walter

DEBUTS TOOLING MACHINE AT GRINDINGHUB 2022

Walter (United Grinding Group) will introduce the latest addition to their machine lineup at the GrindingHub 2022 exhibition: the compact HELITRONIC G 200 tool grinding machine. GrindingHub 2022 runs from May 17–20, 2022 in Stuttgart, Germany, and Walter will be exhibiting in Hall 9, Booth A50. The latest HELITRONIC will also make its North American debut at IMTS 2022.

In a floor space of less than 2.3 square meters (24.8 square feet), the HELITRONIC G 200 offers tool grinding and resharpening of rotationally symmetrical cutting tools ranging from 1 to 125 mm (0.039" to 4.92") in diameter with a grinding wheel up to 150 mm (5.91"). The HELITRONIC G 200 can accommodate a maximum tool length of 235 mm (9.25") and a tool weight of up to 12 kg (26.45 lbs).

The ergonomic design integrates a swiveling multifunction touch panel with a 21.5" monitor, facilitating easy operation and accessibility to the working area. A low-vibration solid mineral cast bed and C-frame construction offers high damping capabilities and thermal stability resulting in maximum grinding precision. The rotating A and C axes are equipped with torque motors. The HELITRONIC G 200 uses HELITRONIC Tool Studio grinding software from Walter.

A loading system is also available where the "Top Loader" is directly integrated into the work envelope of the machine for easy access and requires no additional floor space. Suitable for tools from 3 mm to 16 mm (0.118" to 0.63") in diameter, the maximum tool capacity of the loading system up 500 tools for tools with a 3 mm (0.118") diameter. The Top Loader uses Walter-standard robot pallets and automated electrical teaching.

grinding.com

Jorgensen

INTRODUCES FLEXFILTRATION LINE

Jorgensen Conveyor and Filtration Solutions has introduced its new FlexFiltration line that also includes the company's new Flex G Series of modular filtration systems. The new cost-effective systems feature pre-engineered modules that ensure fast, easy and flexible filtration system configurations for practically any filtering application.

FlexFiltration systems efficiently remove fine chips and grinding sludge to achieve coolant clarity down to 10 microns or less. They are especially well suited for challenging applications involving materials ranging from cast iron, steel and aluminum to composites and plastics.

Jorgensen has developed several pre-engineered base configurations that allow customers to quickly construct a FlexFiltration system specific to coolant-flow requirements. To further match the system to the intended application, the company offers a range of system tanks. These include standard or low-profile versions along with an optional stainless-steel tank that makes the new FlexFiltration system ideal for machine tool OEMs and end users alike. Other modular options that complete a system include high-pressure pumps, auxiliary pumps, tramp oil skimmers, coolant chillers, heat exchangers, liquid level sensors, temperature sensors and the ability to control/interface with existing pumps and other equipment.

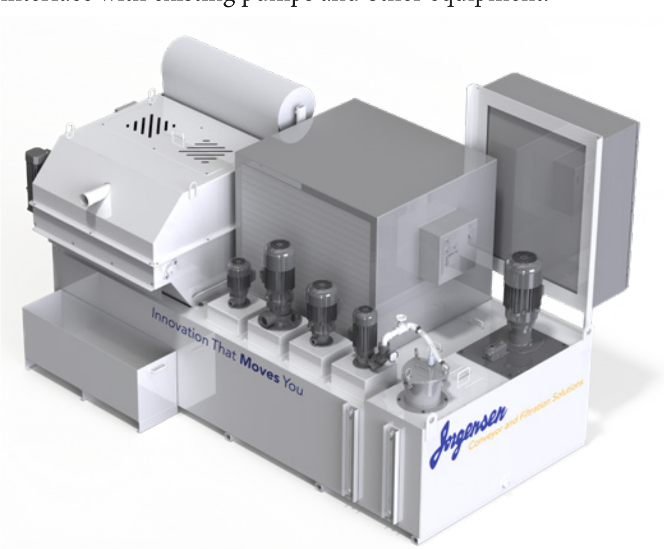

"With the introduction of the FlexFiltration system, Jorgensen further expands its wide range of product offerings that positions us as a leading and single-source provider of conveyor and filtration systems for many different machine tool platforms and models," said Karl Kleppek, director of sales and marketing at Jorgensen. "Our goal is to always provide our customers with modern technologies developed to meet their specific filtering application needs."

jorgensenconveyors.com

3M Technologies

ADDRESS THE E-MOBILITY TREND

The automotive industry is evolving. The trend toward more electromobility is also changing the way cars are being manufactured. In some cases, this has a serious impact, not only on automakers themselves, but also on suppliers. Jürgen Hechler, Global Application Engineering Leader at 3M, is nevertheless confident: "We expect the demand for high-precision abrasives to continue to grow, despite the discussion about electromobility." Among other things, 3M supplies the automotive industry with abrasives for machining gears and shafts.

More and more electric

The share of electromobility is increasing. Between 2016 and 2020, the number of registered electric cars rose from 2.15 million to almost eleven million vehicles *(source: Center for Solar Energy and Hydrogen Research Baden-Württemberg (ZSW))*. By 2030, experts believe that the share of newly registered hybrid and fully electric vehicles worldwide will exceed the 50 percent mark.

Fewer components

"Generally, transmissions and the entire powertrain of purely electric vehicles are simpler than in cars with internal combustion engines. The elimination of the combustion engine and a significant reduction in the size of the transmission mean that fewer components are required. But the quality standards for the individual components increase substantially. Transmissions for electric vehicles have particularly high standards for quality, especially in terms of profile accuracy and surface quality for gears," says Hechler. "In order to increase the efficiency in driving comfort, noise development and driving range in electric vehicles, automotive manufacturers place the very highest demands on ground surfaces in gear manufacturing. The aim is to transmit high torque with low noise at the smallest possible proportions, which in turn increases the demands on the geometry and quality of the components." For this reason, highest profile and flank line accuracies and flawless surfaces are required. For an abrasives manufacturer like 3M, which supplies the automotive industry with grinding wheels for machining these components, this means adapting to the market.

Higher demands

"In the future, demands for abrasives will increase significantly," Hechler explains. This means that in addition to more expertise in application technology, new solutions will be required to meet the increased demands of automotive manufacturers — solutions that 3M is currently developing. One such result is the newly developed ceramic grinding wheels of the 3M Nano 2.0 and 3M Nano+ series with the innovative bond series V450 & V470, which achieve higher performance in profile flank line and surface quality.

Less bonding

Bonding does not grind. Bonding is the unloved ingredient holding together the individual components of the grinding wheel to produce a solid homogeneous

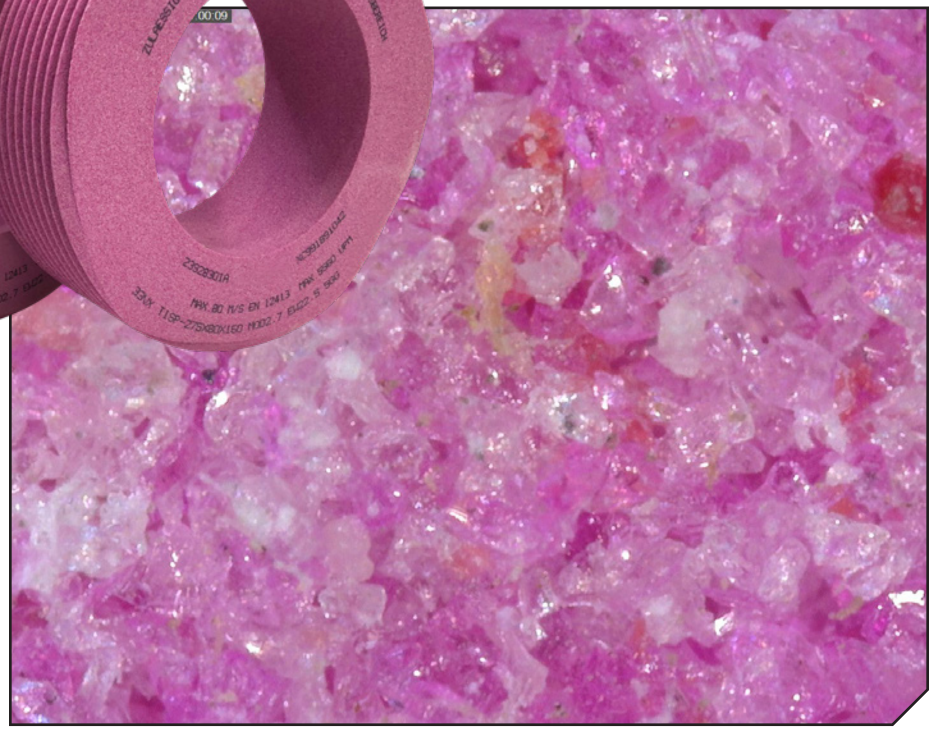

structure. However, the bond also creates pressure and friction, which can subsequently cause thermal damage to the component. The new 3M V450 & V470 bonds allow a significant reduction in the amount of bond required in the grinding wheel while increasing the amount of abrasive grit and maintaining the same grit retention force. "By reducing the amount of bond in the grinding wheel, you prevent these thermal stresses. At the same time, you create more space for the abrasive grains to achieve improved performance of the wheel throughout its entire life cycle," says Hechler. The result is grinding wheels that produce finer profiles and surfaces with increased metal removal rates, longer tool life and reduced thermal stress. "3M Cubitron II grinding wheels are the benchmark for us when it comes to grinding performance. If, in the case of smaller modules, particular importance is placed on surface quality with increased requirements for contact ratio and profile accuracies well below ffα 2.0 μm, 3M Nano 2.0 and 3M Nano+ grinding wheels are the better choice," says Hechler. Nano 2.0 grinding wheels offer good performance in virtually all applications and on all common machine types at an attractive price-performance ratio. Nano 2.0 fine grinding wheels in grit size 150 mesh are the right choice for surface finishing applications with required Rz values below 2 μm and dimensional accuracy. Nano+ wheels with Precision Shaped Grain (PSG) are particularly high-performance and offer the highest dimensional accuracies and process stability for demanding geometries at the tooth tip and root in the module range 0.6 to 4.0. Nano 2.0 Duowheel grinding wheels for use in fine grinding or polishing of gears complete the range. "We are therefore ideally equipped to meet the increased demands of manufacturers," says Jürgen Hechler.

The grinding wheels are manufactured at the 3M plant in Villach, which was rebuilt and extensively modernized only a few years ago after a major fire. "We always have the right product for every requirement in stock and can deliver quickly, and for all common machine types," says Hechler. In the meantime, 3M Nano products are being used successfully by a large number of major automotive manufacturers and suppliers. However, according to Hechler, 3M is already thinking ahead: "The demands on abrasives will continue to increase. And the geometries of the components will also become more complex. In addition, manufacturers are placing ever greater value on long service lives for the abrasives used." According to Hechler, the next step and next challenge is "superfinishing" with vitrified bonded abrasives — in other words, polishing for even greater dimensional accuracy and even finer surfaces, cost-effectively and with process reliability.

At IMTS 2022 in Chicago from September 12–17, visitors can see the benefits of the new 3M Nano grinding wheels for themselves at 3M's booth (East Building, Level 2, Booth 121321).

go.3m.com

For Related Articles Search

grinding

at www.geartechnology.com

The Numbers Game

Nanofluid improves machine performance one particle at a time

Matthew Jaster, Senior Editor

There's a complacency some machine operators can contract over time when presented a new product or machine tool workaround. These new advancements don't necessarily frighten, it's more a case that when an operation works well it's advantageous to leave well enough alone. While many engineers prefer to keep things simple, safe and risk-free, occasionally a new technology offers a unique opportunity to increase productivity.

Tool-X is a nanofluid that changes the characteristics of existing metalworking fluids by 'manipulating' speeds, feeds and metal removal rates using nanotechnology. The science behind Tool-X can potentially change metal cutting dynamics, improve surface finishes and extend tool life. The backstory of this technology is just as fascinating as its production results.

Tool-X is a nanofluid that changes the characteristics of existing metalworking fluids by 'manipulating' speeds, feeds and metal removal rates.

What's a Nano-Onion?

There's a specialized group of scientists and engineers that think on a microscopic level—atoms, molecules, your basic nanotechnology fundamentals. Jim English, president of Tool-X, knows a thing or two about trying to explain the benefits of nanotechnology to potential customers in manufacturing.

"First, it's extremely heavy on the science," English said. "As you're talking about chemical reactions at the microscopic level to a customer you start losing them. The explanation of the process takes longer than the actual process itself."

For this reason, English has been known in the past to refer to the technology as 'magic dust' and prefers to go straight to discussing production gains. A brief explanation, however, works to convey what Tool-X really is and what it can do for a gear shop.

Some of the most fascinating carbon forms in the scientific world are nano-onions. In short, these nanostructures possess great versatility and applicability in areas like medicine, material science, additive manufacturing, plastics, packaging, and nano lubricants. An enlarged photo of a nano-onion looks like an onion sliced right down the middle, hence its name.

"The best way to describe how Tool-X works is the DNA cartoon from the film *Jurassic Park*," English said. "We're taking carbon through a nanoreactor and making different blocks of carbon with different DNA. I tend to use LEGO blocks to explain how we modify and manipulate these carbon blocks."

English said that Tool-X carbon nanoparticles work in both cutting oil and water-based metalworking fluids. The physical properties of the carbon nanoparticles enhance both cutting tool and metalworking fluid performance by reducing the friction between the blade and the chips, conducting heat away from the cutting edge of the tool, removing build-up on the contact surfaces and strain hardening (shot peening) the metal surfaces of the tool. These inert nanoparticles withstand high temperatures and don't break down. To the naked eye, these particles look like dirt, but there's much more going on under the surface.

Tool-X (2003) was originally developed by the U.S. government and brought to the public through a technology transfer program that included the invention of undershirts, sunglasses, synthetic rubber, microwave ovens, GPS and M&Ms — yes, it's true that our favorite hard-shelled candies were given to American soldiers as rations during World War II due to their heat-resistance before appearing in candy aisles.

Another government-led transfer program was Rain-X, the water beading technology that used a hydrophobic silicone polymer to force rain off windshields. This is ultimately the technology that opened the door for Tool-X in manufacturing applications.

Science & Progress

English said that the biggest challenge with nanotechnology is understanding nanotechnology.

"Engineers and scientists need to know the why and the how. How does it work? Why does it work? This is one of the most challenging aspects because they don't understand how a nanofluid like Tool-X can improve productivity," English said.

The lack of nanotechnology education — particularly in manufacturing — plays a role. While Europe and Asia are fully committed to nanotechnology education at the grade school, high school and college levels, it's different here in the United States.

"My son, for example, graduated from college with a biology degree and a teaching certificate. There wasn't a single class on nanotechnology or any mention of the technology throughout his college career. It's discussed more in the medical field, but there's still a disconnect here," English said.

These nanofluids can enhance the thermal conductivity and tribological characteristics in cutting tool applications by reducing friction, lowering tool wear and improving the surface quality of components including gears.

Tool-X has also proven to allow a lower chemical footprint, making it easier for manufacturers to conform to ISO 14001:2015 standards to keep plants clean and healthy for employees. Sustainability and green manufacturing are additional areas the United States tends to trail Europe and Asia.

Nanotechnology, in fact, is one of the key enabling technologies to play a significant role in sustainability in the coming years. It is supported by the United Nations' Sustainable Development Goals in varying fields such as natural sciences, medicine, agriculture, communications and manufacturing.

"Tool-X doesn't smell and it doesn't create bacteria," English added. "We use less additives than other products on the market because we don't need all the additional chemicals."

The EPA went after many of the chemicals used in machine shops in the 1990s. This continues today as new regulations overhaul rules governing thousands of chemical products for consumers, manufacturers and scientists alike.

"Chemists looking to blend new formulas and create new compounds are running out of options. How many tricks do they have left up their sleeves?" English asked.

Tool-X in the Field

For a better understanding of the benefits of this nanofluid, we examined two separate case studies — one for a manufacturing plant in Michigan currently using the product and the other from a hobbing operation at General Motors.

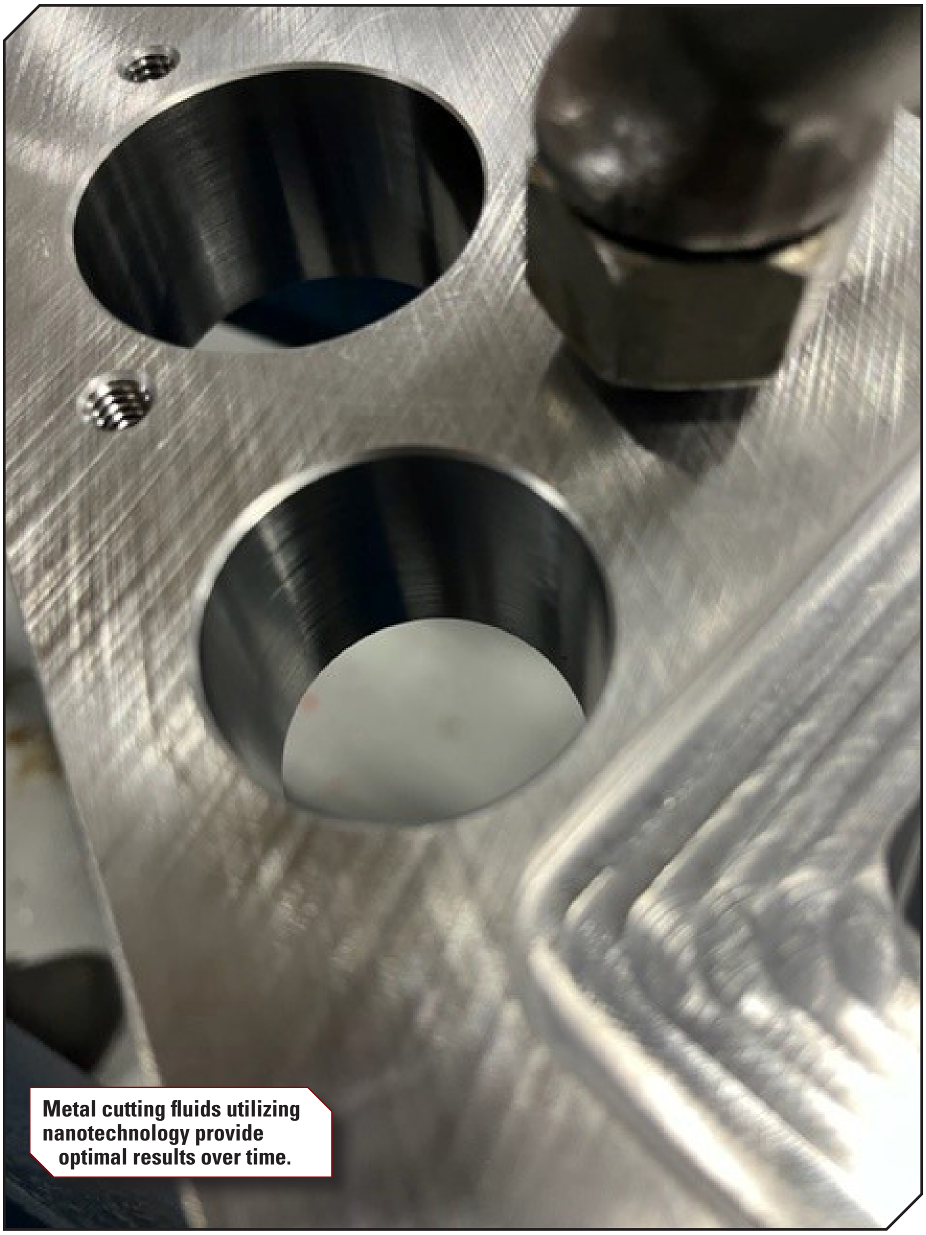

Metal cutting fluids utilizing nanotechnology provide optimal results over time.

4M Aerospace Operation

4M Industries (Livonia, Michigan) is a precision machine shop serving a variety of industries including aerospace, automotive, medical and weaponry. Due to the critical nature of the components produced at 4M, reliability and consistency are vital to the success of the operation.

"COVID was not a factor in slowing our workload down," said Stuart Palm, production manager at 4M Industries. "In fact, we were busier at the height of the pandemic."

Palm stated that the company does not have a sales team trying to find new customers. "We get pretty much all our new business from word of mouth. They come back because of the consistency of our products and our personnel."

These products are maintained by consistently looking at different ways to improve production on the shop floor. Tim Adams, CNC machining specialist at 4M Industries, was the first person on staff to research the potential of Tool-X.

"I was very familiar with the technology because of Rain-X," Adams said. "We read about Tool-X in a trade magazine and inquired about setting up some tests in our facility. The coolant that was being used prior to Tool-X was not meeting 4M's quality requirements."

Adams said the changeover to Tool-X was easy. "The biggest challenges were cleaning the machines completely prior to the switchover and training. Basically, the entire staff needed to learn how this process was different from past coolants used in our machines."

Once Tool-X was implemented, the company saw immediate results.

4M was able to shave off about 40 percent of its cycle time using Tool-X. The company also saw a significant increase in its milling feeds. "The productivity gains were apparent right from the start," Adams added.

He was also surprised at how clean the machines stayed after using Tool-X versus the previous products. "The chips don't hang-up in the machines and there's no wax buildup. The nanofluid helps maintain machine cleanliness during operation which is a bonus," Adams said.

4M is using the technology on its lathes, band saws and in the company's tapping fluid. Adams said they've been able to keep the same saw blade in operation for over a year. They produce steel, aluminum and stainless-steel components for the aerospace industry using Tool-X.

As previously mentioned, the low chemical footprint and clean attributes of Tool-X are the reasons Adams believes other shop floors should consider implementation.

"We have a sister building across the street running the old coolant on the machines and the smell hits you when you walk in the door. There's almost a constant vapor in the air. Our building is not like that at all," Adams said.

Everything is more consistent now on the 4M machine floor. The tools last longer, the machines run faster and the air is cleaner. It looks nothing like the dirty, grimy, soot-filled manufacturing floors of the past.

General Motors Hobbing Operation

GM utilized Tool-X for a hobbing operation for the manufacture of ring gears. This production ran for three years and eight months. According to English, GM increased tool life from 867 parts per tool to 3,813 parts per tool during this timeframe. Scrap savings decreased by $3,072 per machine with productivity savings of $22,624 per machine. The consistency and predictability of the production lines during the testing period were more than enough to convince executives that the same machines and operations could be upgraded using Tool-X.

In a recent presentation for AGMA's Emerging Technologies webinar series, English examined tool and coolant costs before and after GM utilized Tool-X. The production increase was noteworthy.

4M Industries in Livonia, Michigan chose Tool-X for its cleaning attributes and low chemical footprint.

It's All Chemistry and Mathematics

It's a tough concept in manufacturing to suggest a product improves with longevity. Typically, machine tools need to be upgraded, tools resharpened and oils replaced. This — English reiterated — is where Tool-X can surprise customers.

He said that many issues occur in manufacturing because the oil changes month to month.

"One minute a machine shop is getting its oil overseas, then they run out and they're buying from Alaska, then overseas again. These oils are never the same grades. So, you need an additive package to bring it up to application standards. And then you start the process all over again next month."

Nanofluid — in contrast — performs better the longer it's being used.

"In the GM case study, they couldn't figure out how the numbers improved so much over time," English said. "They thought we were adding something to the mixture. Truth is we set up a thirty-day test and it continued to improve over a period of three years. Greater production efficiency is a nice problem to have. Sometimes a technology comes along that challenges the status quo and suggests it's time for a production process to change."

This brings us back to the gear industry's "if it ain't broke, don't fix it" mentality. It is changing. It's safe to say that the next generation becoming executives appears open to trying new things and improving production processes. The leaders speaking up during webinars, trade shows and shop visits realize the importance of upgrading equipment to prepare for our tech-heavy manufacturing future. Tool-X is another example of a program that started out hush-hush in the government but can now offer significant benefits in gear manufacturing.

"The bang for your buck is actually greater in gear manufacturing than other areas," English said. "Tool-X can provide an alternative to lubricants that are not meeting the demands of five-axis machining, carbide tooling, etc. It's a technology that can benefit all the other new machining technologies that are being implemented in today's machine shop."

tool-x.net

Nanotechnology in Electric Vehicles

Like the charged power suit worn by Black Panther of Marvel Comics, UCF researchers have advanced NASA technologies to develop a power suit for an electric car that is as strong as steel, lighter than aluminum and helps boost the vehicle's power capacity. The suit is made of layered carbon composite material that works as an energy-storing supercapacitor-battery hybrid device due to its unique design at the nanoscale level. The development could have applications in a range of technologies that require lightweight sources of power, from electric vehicles to spacecraft, airplanes, drones, portable devices and wearable tech.

"Our idea is to use the body shells to store energy to supplement the power stored in batteries," says study co-author Jayan Thomas, the team leader and a professor in UCF's NanoScience Technology Center and Department of Materials Science and Engineering. "The advantage is that this composite can reduce the weight of your car and increase the miles per charge," he says. "It is as strong as or even stronger than steel but much lighter."

The material, when used as a car body shell, could increase an electric car's range by 25%, meaning a 200 miles per charge vehicle could go an extra 50 miles and reduce its overall weight. As a supercapacitor, it also would boost an electric car's power, giving it the extra push, it needs to go from zero to 60 mph in 3 seconds.

"This application, as well as many others, could be on the horizon one day as the technology advances in its readiness level," says Luke Roberson, study co-author and a senior principal investigator for research and development at NASA's Kennedy Space Center.

These materials could be employed as frames for cube satellites, structures on off-world habitats, or even as part of futuristic eyewear, such as mixed and virtual reality headsets.

"There are lots of potential infusion points within the economy as well as for future space exploration," Roberson says. "This is, in my mind, a huge advancement of the technology readiness level to get us to where we need to be for NASA mission infusion."

On cars, the supercapacitor composite material would get its power through charging, like a battery, as well as when the car brakes. "It's charge-discharge cycle life is 10 times longer than an electric car battery," Thomas said.

The materials used are also non-toxic and nonflammable, which is very important for passenger safety in case of an accident, he says.

"This is a huge improvement over past approaches that have suffered from issues with toxic material, flammable organic electrolytes, low life cycles or poor performance," Thomas said.

Due to its unique design that uses multiple layers of carbon fiber, the material has significant impact and bending strength, essential for withstanding an auto collision, as well as significant tensile strength.

To construct the material, the researchers created positively and negatively charged carbon fiber layers, that when stacked and attached in an alternating pattern, create a strong, energy-storing composite.

Nanoscale graphene sheets attached on the carbon fiber layers allow for increased charge storing ability, while metal oxides deposited on attached electrodes enhance voltage and provide higher energy density. This provides the supercapacitor-battery hybrid with its unprecedented energy storage ability and charging life cycle, Thomas says.

ucf.edu
nano.gov

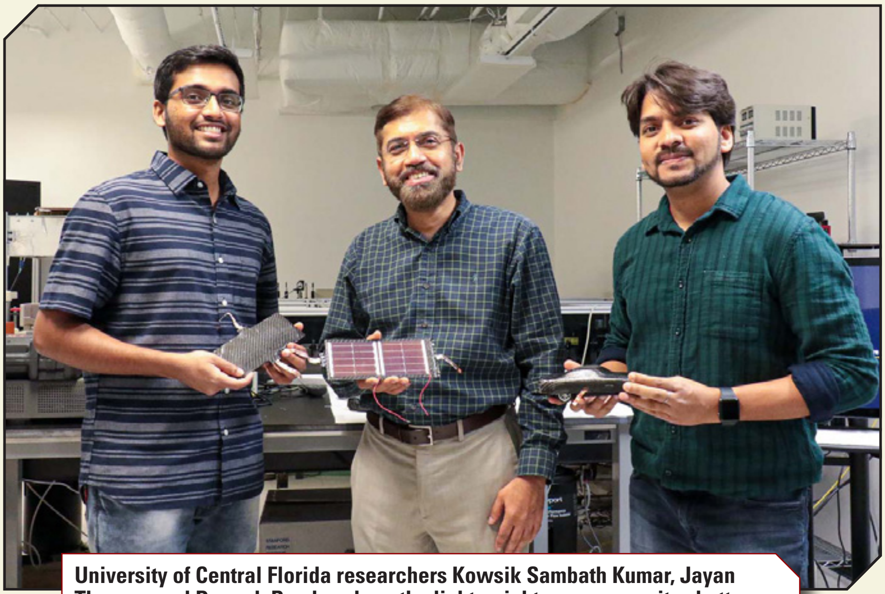

University of Central Florida researchers Kowsik Sambath Kumar, Jayan Thomas, and Deepak Pandey show the lightweight, supercapacitor-battery hybrid composite material they've developed. Kumar and Pandey are UCF doctoral students, and Thomas is a professor in UCF's NanoScience Technology Center and Department of Materials Science and Engineering.


SEPT. 12-17, 2022 • MCCORMICK PLACE, CHICAGO
FIND
IT

Making Gear Grinding Transparent

A process monitoring system brings definition to the undefined

Dr. Christian Dietz and Walter Graf, Reishauer AG, Switzerland

According to the German DIN 8589 standards, the definition of grinding is "a machining process with geometrically undefined cutting edges." That definition, while true in principle (with respect to the intrinsic structure of a grinding wheel), would be false in practice if it were to suggest that grinding is an imprecise process. For example, continuous generating grinding has proven the most productive process for hard-finishing high-precision cylindrical gears; a process based on a dressable, vitrified bonded, threaded grinding wheel called a grinding worm. A process monitoring system (PMS), such as Reishauer's Argus, stabilizes a machining process even as complex as continuous generating gear grinding.

By evaluating dressing and grinding intensities through real-time analytics and proven algorithms, each ground gear's dressing and grinding data are captured and stored in a database where they remain entirely traceable. The PMS renders quantitative data transparent and then uses predictive analytics to make qualitative modifications. This technology helps lead toward zero-defect production, greater precision, and definition of those "undefined cutting edges." The PMS offers comprehensive data analysis possibilities with stored and tracked process and tooling data and individual workpiece identification via DMC (dot matrix code). Preset evaluation limits in the software govern the process interaction and trigger the automatic removal of workpieces that fall outside the set limits.

Continuous Generating Grinding

Continuous generating grinding uses a grinding worm which ensures grinding never takes place in the same spot. Only freshly dressed and unused abrasive grits determine the material removal and the generated gear profile. High-precision diamond rolls profile the worm to maintain constant high-quality manufacture of the gear profiles. This generating process delivers consistent accuracy at high production volumes. However, due to the high output, the use of in-process measuring probes is impossible because gear grinding's axis movements create rapidly changing contact conditions between the grinding wheel and the workpiece. The wheel generates concomitant force vacillations and features a higher degree of complexity than what is found in cylindrical or surface grinding.

Grinding Process Monitoring

One of the essential features of the generating grinding machine is the high output within a short period. For example, for automotive transmissions, grinding cycle times range from eight seconds for small pinions to one minute for ring gears. For this reason, not all ground parts can be measured by coordinate measuring machines (CMMs) due to the measurement times being much higher than the grinding times and the prohibitive costs this would incur. For this reason, the automotive gear industry relies on sample measurements, which represent only a tiny fraction of the total manufacturing lot, generally not higher than five percent.

The continuous grinding process is considered stable and robust as repeated diamond dressing, and the traversal during grinding guarantees a consistently high level of quality. However, as gears are subjected to ever-increasing quality demands, new testing methods are called for that allow constant monitoring of the grinding process. The sample testing processes used in the automotive gear industry run the risk that unsatisfactory gears may end up inside transmissions. Furthermore, the tactile measuring methods of CMMs are, as a rule, not capable of picking up surface variations on gear flanks that may cause detrimental NVH issues in transmissions.

If the grinding intensity generated during the machining process is used as an evaluation criterion, the risk of introducing workpieces of insufficient quality can be eliminated. Real-time analysis

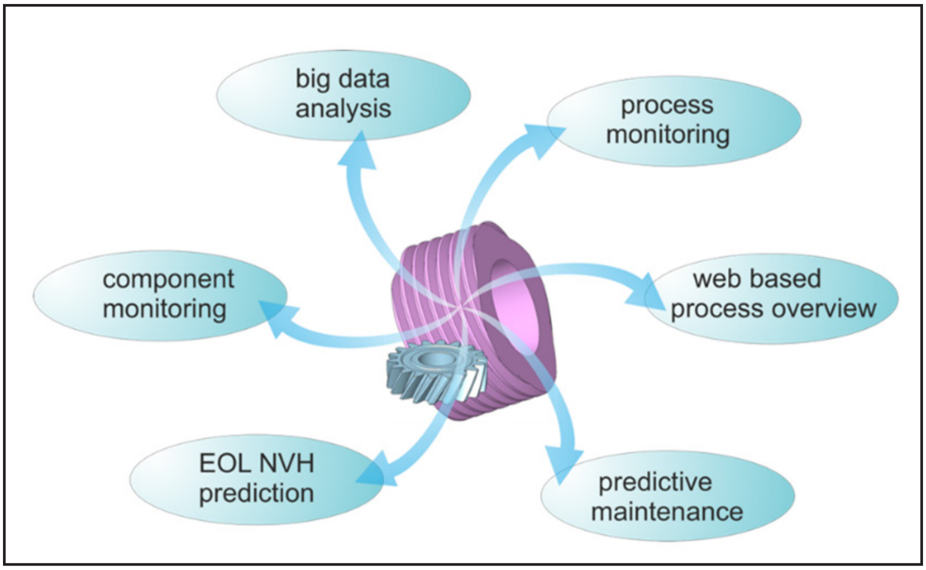

Elements of the process monitoring system.

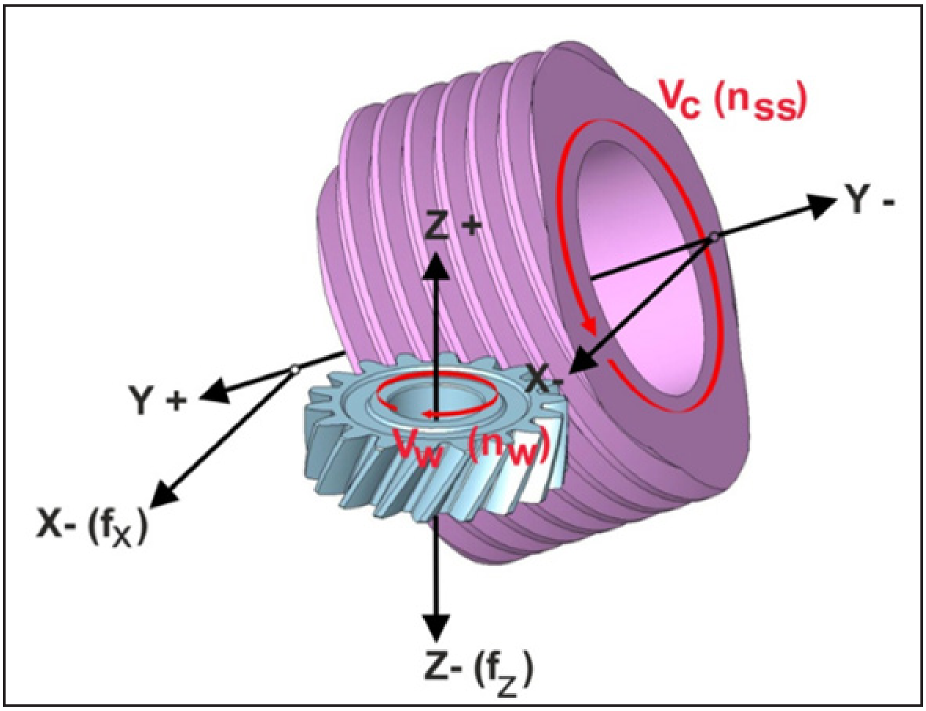

Axes configuration and kinematics of a continuous generating grinder.

of the intensity signal identifies a faulty workpiece during the grinding process if the set signal values have been exceeded. This method translates into a de facto checking of all workpieces in that it allows for faulty workpieces to be automatically identified and removed from the manufacturing process. Reoccurring defective workpieces trigger a systematic error that stops the grinding process and sends a corresponding error message to the operator.

Exceeding the grinding intensity tolerances could be a result of too much or too little grinding stock, hardness distortions, or excessive out-of-roundness from the premachining process. The PMS has integrated sensors to check the dimensions of the premachined gear parts, and excessive out-of-roundness or cumulative pitch errors either lead to an additional grinding stroke or the rejection and removal of the workpiece if the PMS determined additional grinding strokes would not produce a good part.

Grinding intensity is a force-based model — used to calibrate and standardize the grinding process — that continually evaluates the changing chip forming zone, grinding wheel diameter, variations in wheel rpm, and lever ratios across the wheel width in relation to the spindle bearing. This standardization and calibration make it possible to set very narrow limits that result in a high-resolution error evaluation. Even small force vacillations can be detected and automatically checked during the process.

The grinding intensity shows if a worm maintains a consistent cutting performance across its entire width and usable diameter. As a rule, operators evaluate grinding wheels subjectively as empirical data is unavailable. The inhomogeneous hardness variation can only be indirectly assessed via deteriorating gear flank profiles, even though this deterioration may have other causes. The PMS allows the hardness gradient across the grinding wheel width and the changing diameter to be made visible, measurable, and classified.

The grinding intensity also offers an insight into the out-of-roundness levels of clamping fixtures or roundness deviations of the premachined workpieces. For a straightforward interpretation of the dynamics effects of the out-of-roundness of the workpieces on the grinding intensities, the PMS uses proven algorithms to process the time signals captured by the measuring sensors. Using these intensities offers several significant advantages to the operator. The simple interpretability ensures that the analysis of even a complicated process no longer requires the services of highly trained and expensive specialists.

Additionally, even high data volumes generated by large production lots can be visualized. Academic studies are often based on time and frequency analysis of vast data sets with storage reaching several gigabytes. The system's scalar format of the data parameters makes the graphical representation easy, even with thousands of measured data points. Moreover, the system does not require specific evaluation software and hardware. It can be operated with a simple web application on standard web browsers. Given the small data size, it can be transferred any time via the internet or internal networks, even on networks of small bandwidths, and can be efficiently uploaded or downloaded.

The application of this PMS has significant economic benefits. Besides monitoring geometrical inconsistencies, detecting grinding burns is essential to ensure stable production conditions. Grinding burns must be avoided at all costs. Therefore, one of the most common strategies to prevent thermal damage is to reduce feed rates, as thermal damage thresholds are unknown. However, suppose the grinding intensities are calibrated on ground components and proven free of thermal damage. In that case, the process can be optimized with higher feed rates and lower shifting rates. This process optimization leads to shorter grinding cycle times and increased tool life of grinding wheels and diamond rolls, translating into better process economics. Furthermore, as mentioned in the introduction, the principal aim of the process monitoring system is to achieve zero-error production.

Dressing Process Monitoring

The dressing of grinding wheels is of the highest importance for all grinding processes, and the continuous generating gear grinding process is no exception. The rotating profiled diamond dressing roll transfers the precise profile into the threaded wheel and sharpens the grinding wheel's grains to ensure sufficient cutting ability. The complete tooth form is created by a generating movement between the threaded wheel and the gear's movements relative to each other. Even the slightest error in the diamond roll profile is transferred as a mirror image onto the gear profile. Should the diamond roll be blunted by wear, the threaded grinding wheel will in turn be blunted—impeding the cutting ability, leading to low removal rates and possibly grinding burn. To address that, the PMS evaluates the dressing process with force indicators that detect wear on the diamond rolls if the dressing forces exceed a set force envelope.

Moreover, if the threaded grinding wheel features one or several sections of breakage along its threads, it may lead to tooth form deviations. Breakage points show up as force vacillations calculated based on dressing intensity signals. Therefore, wheel breakages can be identified and removed by an additional dressing process. If the breakage were excessive, the system would instruct a grinding wheel change.

Industrial practice often replaces diamond dressing tools when a certain number of predetermined dressing cycles, and therefore a given number of workpieces, has been reached. This practice is often independent of whether the dressing tool may have reached its useful service life or not. However, based on dressing intensity and the resulting indicators of diamond wear, the acceptable limit of the bluntness of a diamond

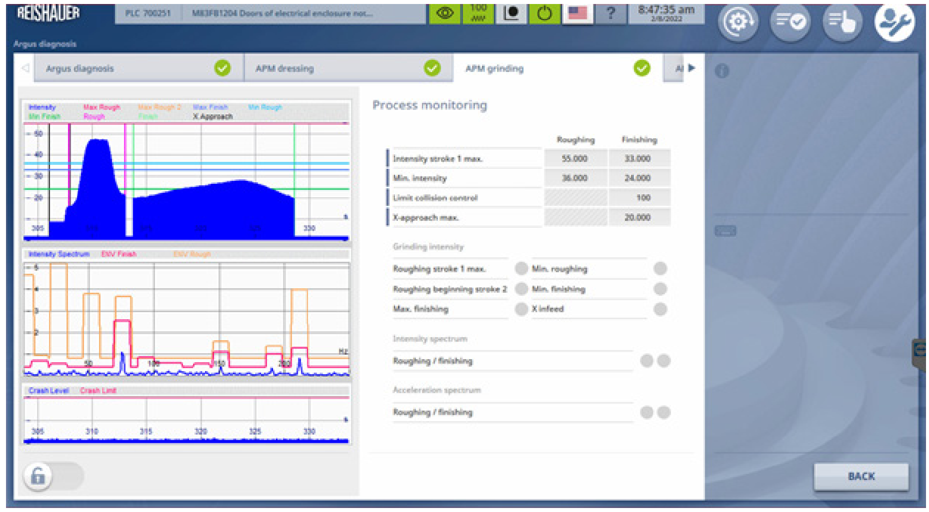

Grinding intensity progression of a two-step roughing and finishing process.

dressing tool can be determined and monitored. For this reason, the useful service life depends on exact measurements and can be utilized more economically over time.

Machine Component Monitoring

Machine tool maintenance is subdivided into two distinct forms: preventive and predictive maintenance. Preventive maintenance is according to a given plan. It is based on time, such as the age of components, guidelines by the component manufacturer, number of axes movements, or other similar established indicators. The PMS is designed to assist in making predictive maintenance decisions that rely on the actual state of components, not on their age or recommended service intervals. On that basis, unnecessary service downtimes and their concomitant costs can be avoided because machine tool services become more predictable and, therefore, more economical. Given stable grinding processes and acceptable premachining, fully functional machine components result in workpieces of higher quality. For this reason, component monitoring significantly contributes to the overall quality assurance process within manufacturing.

Recurring NC testing cycles to measure and evaluate all the relevant grinding machine axes and bearings involved in the process are automatically initiated by the PMS, which enables early detection of electromechanical deviations via sensors that measure vibrations, forces, acoustic signals, and temperature. Maintenance costs are optimized in planning and diagnosis, and some potential EOL gear anomalies may be avoided.

The PMS allows an unbroken recording of all data during the grinding process. Hence, the data can be transferred to a manufacturing execution system (MES), which stores all data free of any time limits. As each workpiece has data sets that include all clamping, dressing, and grinding operations combined with the actual state of each machine component, this may give future insights when the vast amounts of correlated data can be explored with comprehensive data analytics tools. By predicting and analyzing potential NVH issues, the PMS makes complex grinding processes transparent and controllable, carries economic benefits and leads to zero-error production.

reishauer.com/en/technology/argus-monitoring-system

(Additional edits by Aaron Fagan, Senior Editor, *Gear Technology* and *PTE*)

For Related Articles Search
grinding
at www.geartechnology.com

Two New AGMA Publications

Phillip Olson, Director, AGMA Technical Services

AGMA is happy to announce the publication of two new documents: AGMA 925-B22, *Effect of Tribology and Lubrication on Gear Surface Distress*, written by a subcommittee of the AGMA Helical Gear Rating Committee, and, AGMA 943-A22, *Tolerances for Spur and Helical Racks*, written by the AGMA Gear Accuracy Committee.

AGMA 925-B22

AGMA 925-B22 will be a valuable addition to the library of gear and lubricant engineers worldwide. When evaluating a gear design, a logical procedure would be to first calculate macropitting and strength capacity according to AGMA 2101 (or an appropriate application standard), then to use AGMA 925-B22 to determine the risk of surface distress due to lubrication and tribology. AGMA 925-B22 specifically considers the following four surface distress failure types, scuffing, macropitting (using lubrication regimes), micropitting, and wear.

AGMA 925 began as an Annex in the 1995 edition of ANSI/AGMA 2101. In 2003, it was made into a stand-alone document. Work on the now published "B" version began in 2015. The new edition has 106 pages, greatly expanding on the previous edition's 51 pages. It provides more information on surface roughness and gear mesh lubrication. The calculations for gear mesh temperature have been pulled out of the scuffing calculations and placed into a new Clause 8 to assist with surface distress calculations for micropitting and scuffing. The central film thickness has been updated to include a thermal reduction factor as originally proposed by Gupta. Thermal Properties of Steels, given in Annex L, have been expanded using data from the *ASM Handbook, Volume 1: Properties and Selection: Irons, Steels, and High-Performance Alloys,* 10th Edition. The discussion of micropitting in 11.2 now includes a description and parameters for risk evaluation. Additional changes include clarifying diagrams and corrections from requests for interpretation that have been submitted to the AGMA Helical Gear Rating Committee.

AGMA 943-A22

AGMA 943-A22 is the first AGMA publication to cover spur and helical rack tolerancing since the withdrawal of AGMA 390.03a in 1999, which is when the discussions to create this new document began, but the bulk of the work in writing was completed in the last few years. Racks are a commonly manufactured component by companies big and small. The goal of this document is to give those manufacturers — and all other stakeholders in the industry, such as designers, inspectors, and end-users — a common language to describe the quality of racks.

AGMA 943-A22 differs from AGMA 390.03a in that it uses equations to specify tolerances classes instead of tolerance tables. Also, in AGMA 943-A22, lower AGMA tolerance classes designate higher precision to be consistent with international standards. To avoid confusion, the designator "V" is used when specifying tolerance classes from this document for elemental measurements, and the designator "R" is used when specifying tolerance classes from this document for double flank radial composite measurements. Twelve flank tolerance classes are defined, numbered V3 to V14, in order of increasing tolerance. For composite measurements, twenty tolerance classes are provided, numbered R31 through R50 in order of increasing tolerance.

On behalf of the gearing industry, AGMA would like to extend a sincere appreciation for the participation and the valuable contributions of the following experts. In addition, AGMA would like to especially thank the companies of these experts whose foresight and generosity made their participation possible.

AGMA 925-B22 — AGMA Helical Gear Rating Committee Subcommittee

- Robin Olson of Regal Rexnord Corporation, Subcommittee Chairperson
- John B. Amendola III of Artec Machine Systems
- Michael Blumenfeld of ExxonMobil
- Dick Calvert of Chalmers & Kubeck
- Angeline Cardis of Cardis Consulting
- Robert Errichello of GEARTECH
- William Hankes of A-C Equipment Services
- Amir Kadiric of Imperial College London
- Vanyo Kirov of Caterpillar Global Mining
- Timothy Krantz of NASA
- Mark Michaud of REM Surface Engineering
- Andrew Milburn of Milburn Engineering
- Chris Mileti of The Lubrizol Corporation
- Ernie Reiter of Web Gear Services
- Frank Uherek of Regal Rexnord Corporation
- Jeremy Wagner of John Deere

AGMA 943-A22 — AGMA Gear Accuracy Committee

- Steven Lindley of Regal Rexnord Corporation, Committee Chairperson
- John Rinaldo of Atlas Copco (Retired)
- Nicholas Mazur of Innovative Rack & Gear Company
- Terry Miller of Overton Chicago Gear
- Ernie Reiter of Web Gear Services
- Frank Uherek of Regal Rexnord Corporation
- Christopher Wanasek of Caterpillar Global Mining
- Weiguang Wang of Great Lakes Industry
- Timothy Woodruff of Jet Avion Corporation

For Related Articles Search
standards
at www.geartechnology.com

Defining the Tooth Flank Temperature in High-Speed Gears

John Amendola, John Amendola III and Robert Errichello

Introduction

When calculating the total contact temperature the tooth flank temperature is as significant as the flash temperature.

$$\theta_{\text{total contact max}} = \theta_{\text{flash max}} + \theta_{\text{tooth flank temp}} \tag{1}$$

Scuffing is likely to occur when

$$\theta_{\text{total contact max}} \geq \theta_S \tag{2}$$

where:

θ_S = the mean scuffing temperature

Currently, in AGMA 925-A03, Equation 91 includes the oil supply or sump temperature θ_{oil}. If spray lubrication is employed, the oil supply temperature is multiplied by 1.2. This refers to the oil supply temperature as the oil inlet temperature to the gear unit.

Clause 6.3 of AGMA 925-A03 states, "The tooth temperature may be significantly higher than the temperature of the oil supplied to the gear mesh." This statement cites a publication by Errichello (Ref. 1), which refers to the gear tooth flank temperature measured by Akazawa (Ref. 2).

The question is whether a multiplier of 1.2 is sufficient for all speeds of gears utilizing a spray lubrication system varying from relatively slow speed gears with pitch line velocities (PLV) < 35 m/s to high-speed gears with PLV up to 200 m/s.

The field referenced examples used in 19FTM24 (Ref. 3) are high-speed units in operation in the field. See Table 1 for a summary of application data. These units provide data for assessing scuffing risk according to three methods: MAAG "63," ANSI/AGMA 6011-J14, Annex B and AGMA 925-A03. Two additional referenced documents, by Akazawa (Ref. 2) and Martinaglia (Ref. 4) report on testing results of single helical high-speed gears that both confirm the gear tooth flank temperatures increase with PLV. These results are compared in Table 4 The steeper slope with increasing PLVs from Martinaglia's paper (Ref. 4) could be caused by gears with lower helix angles and wider face width's having higher axial pumping velocities.

To fully understand the contents of this paper the reader is encouraged to refer to the earlier paper 19FTM24, a version of which also appeared in the March/April 2020 issue of *Gear Technology* (see *www.geartechnology.com/19FTM24* to download the article). The reference data in this paper is based on extensive experimental data listed in the bibliography.

The objective of this paper is to improve the methodology for determining the tooth flank temperature. Two methods are proposed for assessing scuffing risk when applying AGMA 925 for high-speed gears. Both methods provide similar results.

A Brief Review of Scuffing

- When gears are subject to highly loaded conditions and high sliding velocities, the lubricant film may not adequately separate the surfaces. This can cause localized damage to the surface of the gear tooth flanks called "scuffing." Scuffing exhibits itself as a dull matte or rough finish usually at the extreme end regions of the contact path or near the points of a single pair of teeth contact resulting in severe adhesive wear.
- Scuffing is not a fatigue phenomenon and it can occur instantaneously. The risk of scuffing damage varies with the material of the gear, the lubricant being used, the viscosity of the lubricant, the surface roughness of the tooth flanks, the sliding velocity of the mating gear teeth under load and the geometry of the gear teeth.
- Any changes in any of these factors can alter scuffing risk.

Calculation Methods for Determining Tooth Flank Temperature θ_M

The calculation methods for θ_M given herein were each derived from the DIN 3990-4 Standard.

The original calculation for determining θ_M, given in DIN 3990-4, is based on test stand gearboxes in the FZG laboratory. PLV was reportedly limited to 15 m/s.

DIN 3990-4 (flash temp. method)

$$\theta_M = X_S(\theta_{oil} + 0.47\,\theta_{flmax}) \tag{3}$$

where:

$X_S = k_{sump}$ is 1.2 for spray bar lubrication

The equation can be rewritten:

$$\theta_M = k_{sump}(\theta_{oil} + 0.47\,\theta_{flmax}) \tag{4}$$

Note: $\theta_{Bmax} = \theta_M + \theta_{flmax}$

ISO 6336-20

ISO adopted a modified version of the DIN formula as follows:

$$\theta_M = \theta_{oil} + 0.47\,(X_S)\,(X_{mp})\,(\theta_{flm}) \tag{5}$$

where:

θ_M is Tooth flank temperature
θ_{oil} is Oil inlet temperature
X_S is 1.2 for spray lubrication
X_{mp} is 1 for single mesh gears
θ_{flm} is the average flash temperature (SAP–EAP)

Note: SAP = start of active profile; EAP = end of active profile.

This resulted in:

$$\theta_M = \theta_{oil} + 0.564\,(\theta_{flm}) \tag{6}$$

AGMA 925-A03 (Ref. 5)

AGMA 925-A03 had applied the DIN 3990-4 formula with a single value for k_{sump} and multiplied through the equation, which

Table 1 Data table, Field Referenced Inputs

Ref.	Est hrs	helical	type	*a* (mm)	*b* (mm)	*v'* (m/s)	kW	input (rpm)	output (rpm)	module	Z_1/Z_2	*b/d*	*β*
1	>200k	single	increaser	400	236	142.0	10,515	4,831	11,406	6.5	36/85	1.07	10°
2	120	double	decreaser	360	228	112.0	7,915	8,476	4,573	5.5	41/76	0.90	26°30′
3	175k	single	increaser	250	120	118.3	4,096	6,840	13,310	4.5	37/72	0.71	10°
4	160k	single	decreaser	580	502	109.3	37,286	4,670	2,927	6.25	47/75	1.12	10°
5	180k	single	increaser	520	352	142.1	22,670	3,428	10,933	6.5	37/118	1.42	11°
6	200k	single	increaser	780	255	123.0	13,500	1,775	9,951	7.0	33/185	1.08	10°30′
7	150k	double	increaser	610	370	92.7	16,406	1,800	7,636	6.0	33/140	1.59	31°20′
8	150k	single	increaser	509	323	72.6	12,304	1,800	5,606	6.9	35/109	1.31	10°
9	120k	single	increaser	600	270	88.1	9,694	1,800	7,582	5.9	37/163	1.22	10°
10	200k	double	increaser	270	140	43.7	570	1,782	11,616	3.4166	19/124	1.95	24°
11	120K	single	increaser	500	347	175.3	31,905	4,786	11,100	6.3	46/107	1.15	13°30′

Note: $\theta_{Bmax} = \theta_M + \theta_{flm}$ where θ_{Bmax} is maximum contact temperature.

Table 2 AGMA-925-A03 Preset Input Parameters

Oil Type:	Mineral VG-32
FZG Load stage:	fail 6
Scuffing temperature θ_s:	177°C
Oil Temperature:	49°C
surface roughness R_a:	0.50 µm
LSF (load sharing factor):	smooth meshing/with profile modification
Thermal Coefficient of Contact for Steel B_m :	13.796 N/[mm s0.5 K]

fixed the multiplier variable for θ_{flm} to 0.56

$$\theta_M = k_{sump}(\theta_{oil}) + 0.56\,\theta_{flmax} \tag{7}$$

where:

θ_{flmax} is maximum flash temperature along (SAP–EAP)

k_{sump} is 1.2 for spray lubrication

This resulted in:

$$\theta_M = 1.2\,(\theta_{oil}) + 0.56\,\theta_{flmax} \tag{8}$$

The equation should have been rewritten:

$$\theta_M = k_{sump}(\theta_{oil} + 0.47\,\theta_{flmax}) \tag{9}$$

However, if k_{sump} is to be treated as a variable then the original DIN formula needs to be applied as shown in Equation 9. The authors consider Equation 91 in AGMA 925-A03 is only valid when $k_{sump} = 1.2$.

Establishing the Oil Inlet Temperature θ_{oil} Using a Variable Multiplying Factor k_{sump}

The $k_{sump} = 1.2$ was reportedly developed using small test stand gears limited to 15 m/s PLV in a laboratory environment. For an inlet temperature of $\theta_{oil} = 49°C$ the multiplying factor of 1.2 results in a supply temperature of $\theta_{oil} = 59°C$ delivered to the tooth flank. This is considerably less when using MAAG and AGMA 6011 Annex B which fixed the tooth flank temperature at 100°C. To equate the use of the DIN 3990/AGMA 925 equation, a $k_{sump} > 1.2$ is required in order to raise the supply temperature to 70°C. This would generally result in a tooth flank temperature of 100°C which is consistent with MAAG & ANSI/AGMA 6011 Annex B. Assessing scuffing risk for high speed gears using AGMA 925 with the current 1.2 multiplier would result in a false assessment of safety.

AGMA 925-A03 applies the k_{sump} factor as a multiplier of the oil inlet temperature $\theta_{oi\,1}$, whereas ISO 6336-20 does not.

For pitch line velocities less than 35 m/s the ISO approach seems logical as it is expected the gear elements would be supported with antifriction bearings. However, above 35 m/s most gear units are installed with hydrodynamic bearings which are lower in efficiency and contribute heat to the housing structure and in turn add heat to the oil supply temperature θ_{oil}. Therefore, for high-speed gears this document uses the original DIN 3990-4 equation.

This document includes data from the field inspections (Ref. 3) shown in Table 1, and instrumented test gears (Refs. 2, 4) shown in Tables 4a and 4c.

Referenced Gears

Test Gear (Ref. 2)

25,000 HP speed increaser   7656/18689 rpm   Single Helical
a: 506.25 mm   *b*: 250 mm   *v'*: 200 m/s
Temperature measurements using embedded thermocouples in the pinion/gear teeth.

Test Gears (Ref. 4)

Various 21-62 MW speed reducers/increasers   Single Helical
21 MW   3000/7625 varying speeds   Single Helical
a: 360 mm   *b*: 300 mm   *v'*: 137 m/s – 148 m/s
Temperature measurements using embedded thermocouples in the pinion
62 MW   2988/1000   Single Helical
a: 1750 mm   *b*: 802 mm   *v'*: 137 m/s
Temperature measurements using imbedded thermocouples in the pinion

All gearsets described in this document are of a single or double helical configuration. Spur gears have not been considered.

Field References (Ref. 3)

Table 1 is a summary of the inspected gear units in field operation with applied data in assessing scuffing risk.

Table 2 lists preset input parameters for the calculations listed in Table 3.

The values of θ_M in Table 3 differ from those given in 19FTM24 (Ref. 3) for the same field references. The values in 19FTM24 (Ref. 3) applied a fixed value for $k_{sump} = 1.2$ using a very high oil supply temperature of 70°C, whereas Equation 10 in this document employs a variable value for k_{sump} with normal oil inlet temperature of 49°C.

The actual measured tooth flank temperatures listed in Tables 4a and 4b are taken from test data (Refs. 2, 4). They indicate k_{sump} increases with increasing PLV. The Table 4a and 4b values were compared to the field references of similar pitch line velocities and a value for k_{sump} was applied to the examples in Table 3 to match the measured values in test data (Refs. 2, 4). The calculated tooth flank temperatures θ_M listed in Table 3 are summarized in Table 4c for comparison with full-size test gears (Refs. 2, 4). The comparison shows comparable θ_M values. They are grouped in stepped values of k_{sump} as follows:

$k_{sump} = 1.0$ for splash lube

= 1.2 for spray lube with gears utilizing antifriction bearings

= 1.35 for PLV 35–50 m/s

= 1.38 for PLV 50–90 m/s

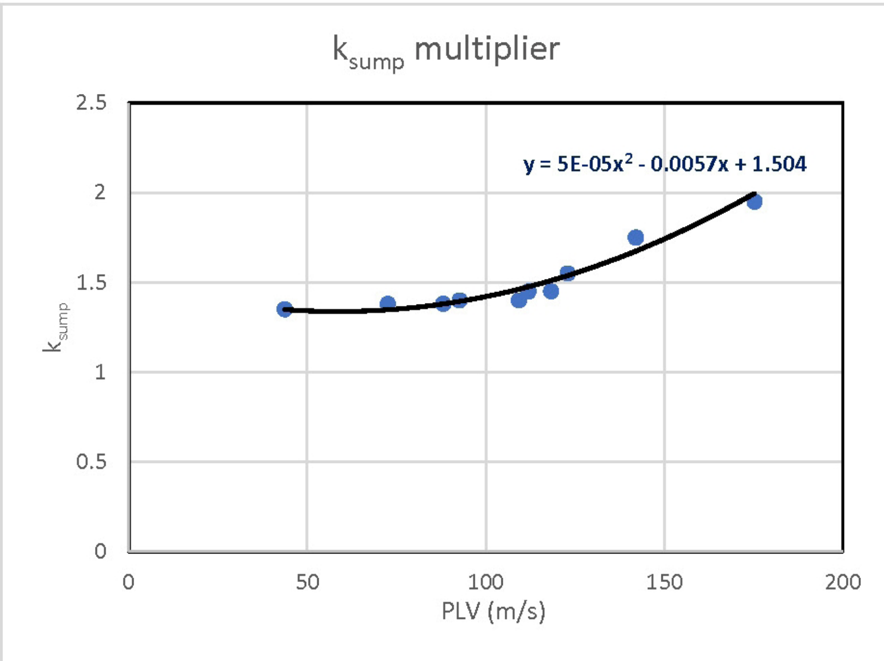

Figure 1

Table 3

v′ range (m/s)	Case	v′ (m/s)	Scuffing risk	Risk	Tooth Temp (°C) θ_m	Flash Temp (°C)	Contact Temp (°C)
k_{sump} = 1.35 (DIN)*							
35≥50	10	43.7	5.0%	low	75.3	14.5	91.5
k_{sump} = 1.38 (DIN)*							
50≥90	8	72.6	5.0%	low	89.1	33.1	122.3
	9	88.1	5.0%	low	80.3	19.6	99.9
k_{sump} = 1.40 (DIN)*							
90≥110	4	109.3	5.0%	low	90.4	33.1	123.5
	7	92.7	5.0%	low	92.9	37.0	129.9
k_{sump} = 1.45 (DIN)*							
110120	2	112.0	5.1%	moderate	96.8	37.8	134.6
	3	118.3	5.0%	low	75.6	6.7	82.3
k_{sump} = 1.55 (DIN)*							
120≥130l	6	123.0	5.0%	low	92.0	22.0	108.1
k_{sump} = 1.75 (DIN)*							
130≥145	1	142.0	5.0%	low	99.2	16.3	115.5
	5	142.1	5.0%	low	108.2	27.4	132.6
k_{sump} = 1.95 (DIN)*							
>170	11	175.3	23.7%	moderate	120.0	26.3	158.3

* k_{sump} calculated per DIN 3990-4 (flash temp. method) per Equation 4

Table 4a

v′ (m/s)	θ_m (°C)
100	80
110	85
120	90
130	95
140	100
150	105
160	110
170	115
180	120
190	125
200	130

4a Note: Measured test gear values (Ref. 2)

Table 4b

v′ (m/s)	θ_m (°C)
100	70
115	85
134	101
145	111
151	117
160	125

4b Note: Measured test gear values (Ref. 4)

Table 4c

Ex. Ref.	v′ (m/s)	DIN (X_s) k_{sump}	θ_m (°C)
10	43.7	1.35	75.3
8	72.6	1.38	89.1
9	88.1	1.38	80.3
4	109.3	1.40	90.4
7	92.7	1.40	92.9
2	112.0	1.45	96.8
3	118.3	1.45	75.6
6	123.0	1.55	92.0
1	142.0	1.75	99.2
5	142.1	1.75	108.2
11	175.3	1.95	120.0

4c Note: field (calculated values) (Ref. 3)

= 1.40 for PLV 90–110 m/s
= 1.45 for PLV 110–120 m/s
= 1.55 for PLV 120–130 m/s
= 1.75 for PLV 130–145 m/s

Values above 145 m/s should be based on field experience or applying the curve in Figure 1.

A plot for k_{sump} versus PLV can be applied as an option to a table as shown in Figure 1.

This curve is based on the references listed in Table 4c resulting in the following equation:

$$k_{sump} = 0.00005(v')^2 - 0.0057(v') + 1.504 \tag{10}$$

Verification of the Calculated Values to Measured Test Values

For further verification, measured values for pinion tooth flank temperatures from Tables 4a and 4b and the calculated values from Table 3 are plotted against PLV in Figure 2. By plotting all values the following averaging relationship can be defined as follows:

$$\theta_M = 0.0021(v')^2 - 0.1188(v') + 77.088 \tag{11}$$

Similar adjustment can be applied to C_w in the formulation used in Annex B of ANSI/AGMA 6011-J14 (Ref. 7).

Table 5 compares the results from Equation 11 for θ_M with those calculated with k_{sump} listed in Table 4c.

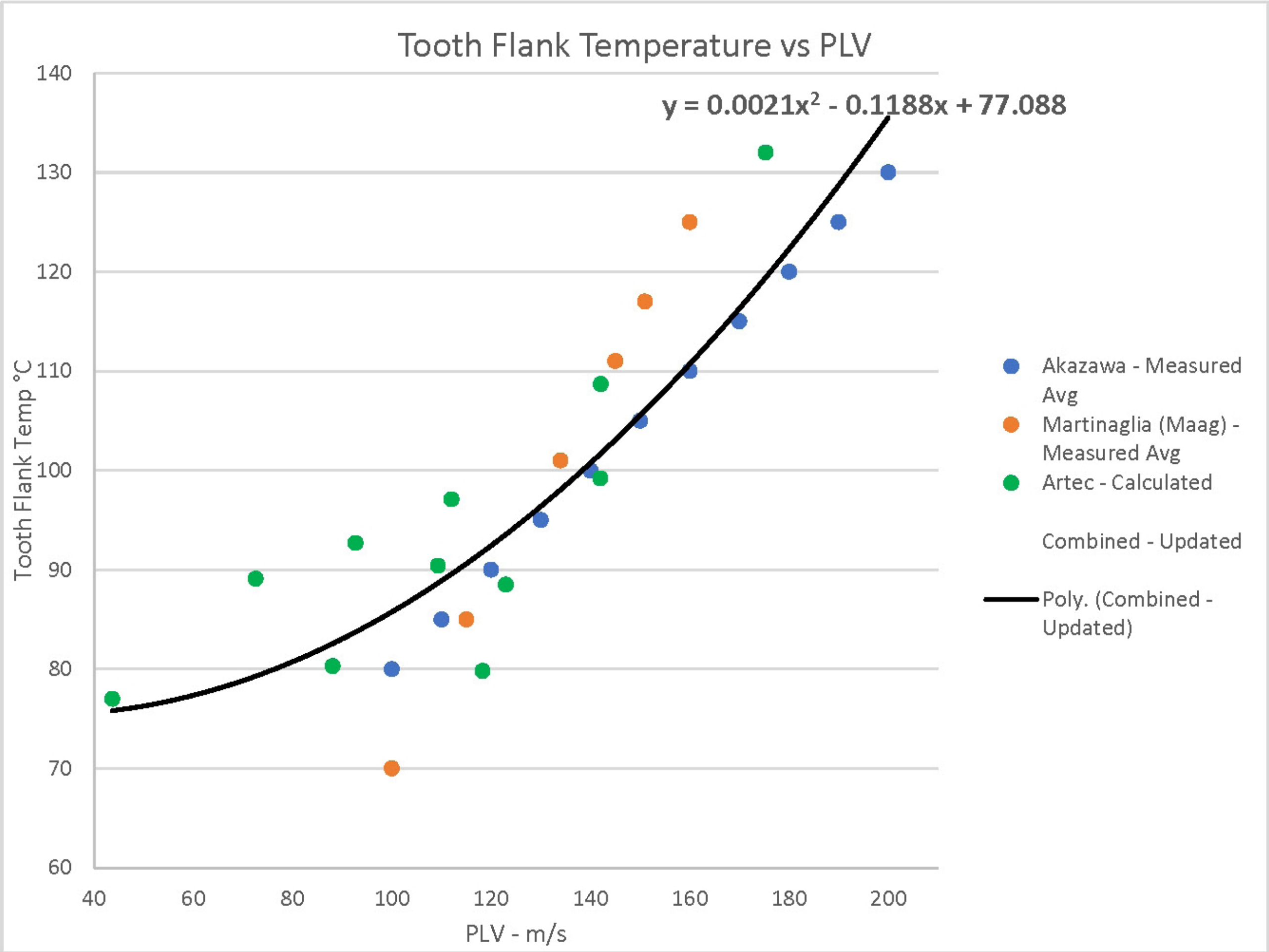

Figure 2

Table 5

Field Ex. Ref.	v' (m/s)	DIN(X_s) for k_{sump}	Equation 10 θ_m (°C)	Equation 11 θ_m (°C)
10	43.7	1.35	75.3	75.9
8	72.6	1.38	89.1	79.5
9	88.1	1.38	80.3	82.9
4	109.3	1.40	90.4	89.2
7	92.7	1.40	92.9	84.1
2	112.0	1.45	97.1	90.1
3	118.3	1.45	75.6	92.4
6	123.0	1.55	92.0	94.2
1	142.0	1.75	99.2	102.6
5	142.1	1.75	108.2	102.6
11	175.3	1.95	120.0	120.8

Table 5a

Field Ex. Ref.	v' (m/s)	ISO 6336-20 X_s	Equation 10 θ_m (°C)	Equation 11 θ_m (°C)
10	43.7	3.88	75.3	75.9
8	72.6	2.58	89.1	79.5
9	88.1	3.41	80.3	82.9
7	92.7	2.54	92.7	84.1
4	109.3	2.66	90.4	89.2
2	112	2.68	97.1	90.1
3	118.3	8.48	75.6	92.4
6	123	4.15	92	94.2
1	142	6.53	99.2	102.6
5	142.1	4.61	108.2	102.6
11	175.3	10.42	120	120.8

These values for θ_M are reasonably consistent. References 2, 6 and 11 are all references where tooth surface distress had been evident. Corrective action was required to arrest the problem.

Note ISO 6336-20 Equation 5 differs significantly from DIN 3990-4 Equation 3 because the oil supply temperature θ_{oil} is not adjusted by X_S values as proposed in Table 3. Therefore, a different set of X_S values described by PLV levels will be required for application with Equation 4. However, in using ISO 6336-20, Equation 11 is applicable.

Using ISO 6336-20 Equation 5 the values for X_S are adjusted for use of the equation.

Equation 5 from ISO 6336-20 produces a scattering of values for X_S versus PLV levels which cannot result in a curve similar to Equation 10. Equation 5 from ISO 6336-20 produces a scattering of values for X_S versus PLV levels which cannot result in a curve similar to Equation 10.

Determining Value for θ_M

Equations 10 and 11 are both suitable equations to calculate a value for θ_M in AGMA 925.

Method A

The value for k_{sump} obtained from Equation 10 can be applied in Equation 9 to obtain a value for θ_M.

Method B

Equation 11 directly calculates θ_M. It should be noted when using this method the applied data is based on oil supply temperatures over a limited range from 40˚C–70˚C. Most of the Table 3 applications had a supply oil temperature of 43°C–55°C. Therefore, the reliability of Method B where a lube oil supply temperature is beyond this range may be somewhat compromised. Furthermore, Method B should only be applied with gears utilizing hydrodynamic bearings. The Table 3 gears employed sump pans to prevent windage affecting the outflow of oil through the discharge port(s). Additional shrouding of the gear rotors that can mitigate tooth flank temperatures is not considered here. Tooth flank temperatures with shrouded gears should be based on field individual field experience.

Factors that Influence Tooth Flank Temperature

In all the high-speed examples discussed, the gears employed hydrodynamic bearings. These bearings are less efficient than roller bearings used in FZG testing. The heat generated in hydrodynamic bearings is significant. Martinaglia (Ref. 4) reported measured values of approximately 30% of the gear power losses was in the bearings. Temperature range as measured in journal bearing RTDs are typically in the range of 70°–90°C. Consequently, the bearing journals absorb heat. The question is, does the energy absorbed by the journals, particularly higher in the pinion, contribute to the tooth flank temperature. During the early Nineties, MAAG developed special turbo gears whereby the gears operated in a near-vacuum. Tests were conducted on a full-sized 65 MW turbo gear (Ref. 8). Temperature measurements in the gearing were recorded for both conventional and near-vacuum modes. The temperature difference was reportedly approximately 40°C lower in the vacuum mode.

It can be stated the requirements to increase the k_{sump} factor in high-speed gears is primarily the result of the operating windage. Martinaglia had suggested, "in especially fast running gears, the frictional heat developed in the bearings also passes via the shaft stub into the pinion body proper." Furthermore, the MAAG HET test results have shown this to be a significant influence. More recently there have been some high-capacity gears designed with a shroud that closely surrounds the gear set. The shroud is externally cooled, thereby minimizing the oil flow required in the gear mesh for lubricating purposes only. This in turn reduces the pumping losses in the mesh resulting in an increase in operating efficiency. This also mitigates the adjustment in the lead modification to compensate for thermal deformation.

There are some variable factors that result in minor differences in the tooth flank temperatures plotted in Figure 2. Length of the tooth face width, size of the module, helix angle of the gear and internal housing dimensions can influence the windage behavior. Test Gear 4 temperature plots are steeper than Test Gear 2 temperature plots most likely due to lower helix angles. These differences have a minor influence on the variations in tooth flank temperatures. There are infinite combinations of these parameters making it difficult to assess their influence on the values of θ_M. This is shown by the varied plots of the field references where these parameters are all from different gearboxes. Nevertheless, PLV has the single largest influence on operating tooth flank temperatures.

However, where windage is low, the number for k_{sump} is lower. The gear References 2 and 4 and "Field Reference 3" indicate there are small changes for the k_{sump} number. For PLV < 35 m/s, k_{sump} may not be less than 1.35. It is not in the scope of this document to evaluate values for k_{sump} where PLV < 35 m/s. The AGMA threshold for high-speed gears applies for pitch line velocity above 35 m/s. The determination of k_{sump} requires additional research where operating PLVs are between 15–35 m/s. Nevertheless, it seems improbable there could be a significant change between $k_{sump} = 1.2$ up to 15 m/s and $k_{sump} = 1.35$ up to 35 m/s.

References 2 and 4 and the Table 3 applications were equipped with hydrodynamic bearings whereas the FZG test gears employed antifriction bearings. Power losses in gears with hydrodynamic bearings may influence the gear tooth flank temperatures from heat absorbed by the bearing journals and transmitted into the main body of the gear elements. Therefore, suggested values for k_{sump} are:

$k_{sump} = 1.35$ for gears where PLVs are < 35 m/s when equipped with hydrodynamic bearings.

$k_{sump} = 1.20$ for gears where PLVs are < 35 m/s when equipped with antifriction bearings.

Note: ANSI/AGMA 6011-J14 references high-speed gears with hydrodynamic bearings. Roller bearings are occasionally used in special cases.

Conclusions

1. AGMA 925-A03 Equation 91 should be limited to PLV < 35 m/s for gears equipped with antifriction bearings.
2. Method A for calculating k_{sump} in Equation 10 should be used to calculate θ_M in Equation 9 and added to AGMA 925.

3. Method B for calculating θ_M using Equation 11 should be added to AGMA 925.
4. The fixed k_{sump} value in AGMA 925-A03 is not suitable for assessing scuffing risk for high-speed gears and will lead to an erroneous value for safe scuffing assessment.

References

1. Errichello, R. *Friction, Lubrication and Wear of Gears,* ASM Handbook, Vol. 18, Oct. 1992 pp. 535–545.
2. Akazawa, M. *Full Scale Test of High Speed, High Powered Gear Unit:* August 18, 1980.
3. Amendola, Amendola, Errichello; *19FTM24 – Calculated Scuffing Risk: correlating AGMA 925-A03, AGMA 6011-J14 and Original MAAG Gear Predictions:* October, 2019.
4. Martinaglia, L. *Thermal Behavior of High-Speed Gears and Tooth Corrections for Such Gears*; Oct. 11, 1972.
5. AGMA 925-A03, *Effect of Lubrication on Gear Surface Distress*; March 13, 2003.
6. API 613-5, *Special Purpose Gear Units for Petroleum, Chemical and Gas Industry Units*. Sec. 2.8.2; December, 2002.
7. ANSI/AGMA 6011-J14, *Specification for High Speed Helical Gear Units*; Annex B, December 19, 2019.
8. Deeg, Thomas; The MAAG High Efficiency HET Turbo gears; 1996.

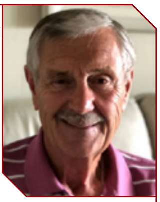

John B. Amendola is an executive officer and chairman of the board and Chairman of the Board of Artec Machine Systems where he has been working for 50 years. Prior employment was with Western Gear, Texaco & Boeing Co. where he operated a full load four square locked torque test stand for helicopter gears. He is currently an active member of AGMA Helical Gear Rating & Lubrication Committees, active chairman of AGMA Enclosed High Speed Units Committee, a member of the US TAG to ISO TC60 and a member of the American Petroleum Institute 613-6 Standards Committee. John holds a Bachelor of Mechanical Engineering from Villanova University and a Master of Science degree in Mechanical Engineering from (NYU) Brooklyn Polytechnic Institute. Amendola is a recipient of the AGMA TDEC Award.

John B. Amendola III, is the president of Artec Machine Systems where he has been working for 29 years. Prior experiences include: 1 year at Maag Gear, Zurich Switzerland, with assembly, testing, field services group for high speed gear applications; and 2 years at SUNY Maritime College, Assistant Professor Engineering Department training of engineering undergrads in Marine/Mechanical operations. He is an active member AGMA Helical Gear Rating Committee and holds a Bachelor of Science in Marine Engineering from Maine Maritime and a Professional Engineering License for Mechanical Engineering. John III also maintains a USCG unlimited license as a senior Marine Engineering Officer and Commander Retired US Navy Reserve.

Robert Errichello heads his own gear consulting firm, GEARTECH, and is founder of GEARTECH Software, Inc. He has over 57 years of industrial experience. He has been a consultant to the gear industry for the past 44 years and to over 50 wind turbine manufacturers, purchasers, operators, and researchers. A graduate of the University of California at Berkeley, Errichello holds BS and MS degrees in mechanical engineering and a Master of Engineering degree in structural dynamics. He is a member of several AGMA Committees, including the AGMA Gear Rating Committee, AGMA/AWEA Wind Turbine Committee, ASM International, ASME Power Transmission and Gearing Committee, STLE, NREL GRC, and the Montana Society of Engineers. He is technical editor for GEAR TECHNOLOGY and STLE Tribology Transactions. Errichello is recipient of the AGMA TDEC Award, the AGMA E.P. Connell Award, the AGMA Lifetime Achievement Award, the STLE Wilbur Deutch Memorial Award, the 2015 STLE Edmond E. Bisson Award, and the AWEA Technical Achievement Award.

Algorithm-Based Optimization of Gear Mesh Efficiency in Stepped Planetary Gear Stages for Electric Vehicles

Christian Westphal, Jens Brimmers and Christian Brecher

Introduction and Motivation

Increasing demands on product performance have led to high demand for optimization in component design. Optimization methods can be used to solve the conflicts between different design objectives. The importance of numerical optimization methods is also increasing in the gear design and is part of different phases of the development process. The gear design is divided into four essential steps, which are necessary for the definition of the macro- and microgeometry of the gears (Ref. 1).

The process shown in Figure 1 starts with the determination of the gearbox topology. The topology is largely derived from the gear ratio requirement between driving and driven components. Methods for optimizing the transmission topology are based on simplified standard calculations and evaluating various transmission topologies. The possible topologies are evaluated concerning their volume, the expected efficiency, and the achievable load-carrying capacity. At this early stage of development, these parameters can only be determined approximately since the macrogeometry of the gears and the shaft bearing system have not been defined yet. With the gear topology selected, the gears can be designed, see Figure 1. The boundary conditions for designing the gear stages, such as the center distance, the gear ratio, and the face width, have been defined in the previous step. A design of gears with a focus on the load-carrying capacity is possible according to ISO 6336 (Ref. 2). If other design objectives are in focus, such as efficiency or excitation behavior, higher-level methods are recommended. With a variant calculation, the selection of a gear geometry corresponding to the requirements is possible. With an increasing number of variation variables, numerical optimization methods can be more target-oriented compared to variant calculations. For the final evaluation of the operational behavior, for example, FE-based methods can be used (Refs. 3 and 4).

In the third step of the gearbox design, further components such as shafts, bearings and the housing are designed, see Figure 1. The transmitted forces and torques are completely defined at this development step. Especially for gearboxes with a high required power density, an iterative procedure within the first three design steps may be necessary (Ref. 1). The last and fourth step of the gear design is the optimization of the tooth contact with a specifically designed microgeometry. The level of detail of the design is the highest in this step, so numerical methods are often used. When designing the microgeometry, manufacturing deviations and load-dependent misalignments can be considered. FE-based variant calculations are suitable for determining an optimal microgeometry. Further optimization potential in this design step is provided, for example, by topological flank modifications (Refs. 5 and 6).

Optimization methods can be usefully applied in every step of the gear design process. Especially for gearboxes with more complex kinematic relationships and additional geometric restrictions that vary depending on the design parameters, as it

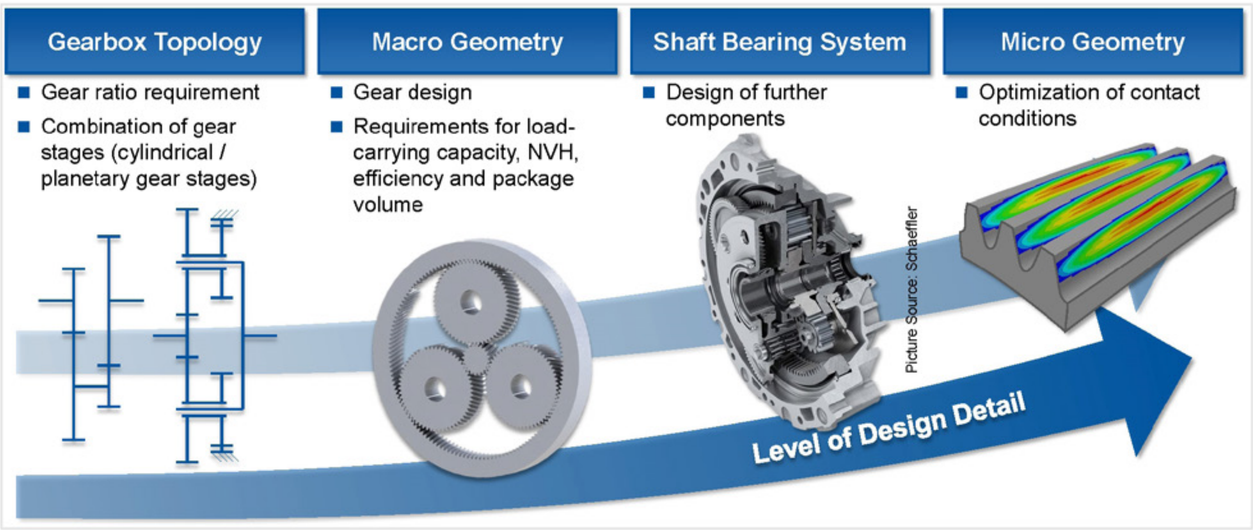

Figure 1 Gearbox Design Process

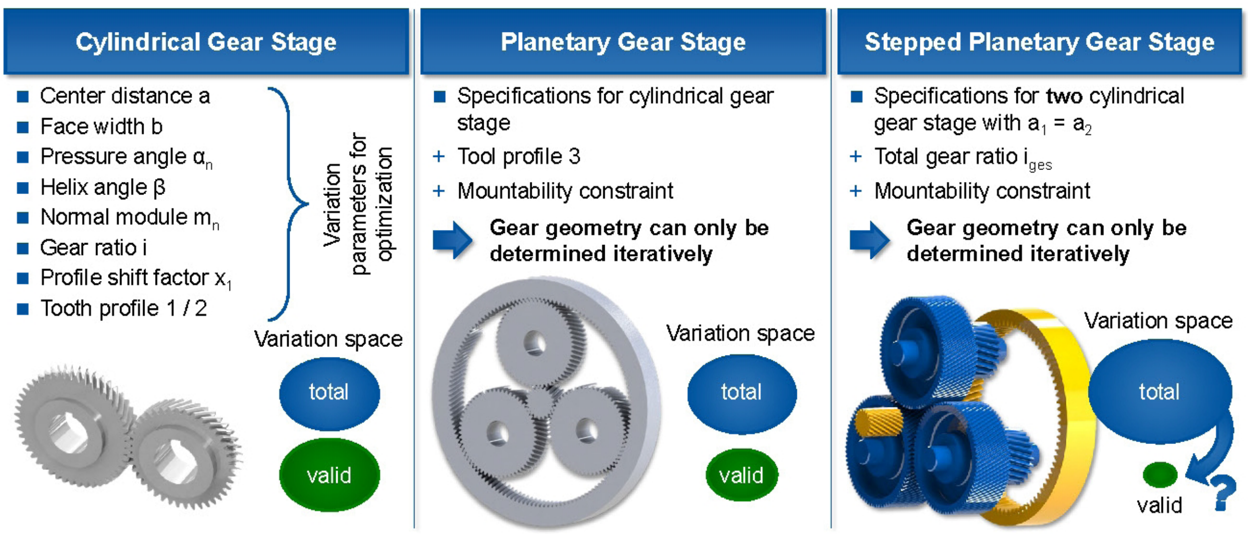

Figure 2 Variation Parameters and Constraints in the Design of Stepped Planetary Gear Stages

is with the case of planetary gear stages, numerical optimization methods can make further potential available.

Design of Stepped Planetary Gear Stages

One of the challenges in the design of automotive transmissions is the combination of high power density, high efficiency, and low noise excitation. With the electrification of the powertrain, the requirements in terms of noise excitation and efficiency increase further. On the one hand, the masking noise of the combustion engine is eliminated, and on the other hand, energy efficiency is mandatory for electric vehicles. To meet these requirements, complex transmission topologies with planetary gear stages are increasingly being used. Advantages of planetary gear stages are, in particular, the short axial length in conjunction with the coaxial alignment of the input and output shafts and the comparatively high gear ratio and power density. To increase the power density and the maximum achievable gear ratio further, stepped planetary gear stages (also called compound epicyclic) can be used. In these, a stepped planet consisting of two rigidly connected gears is used instead of one single planet. The input shaft of the stepped planetary gear stage considered in the following is the sun. The ring gear is fixed to the housing and the output shaft is the planet carrier.

With this gear configuration, ratios between sun and carrier of $i_{SC} \geq 20$ are possible, considering geometric boundary conditions. The stationary gear ratio i0 is calculated according to Equation 1, which describes the gear ratio with a planet carrier fixed to the housing, input on the sun and output on the ring gear. The stationary gear ratio i0 is used to derive the gear ratio i_{SC} of the relevant configuration with the ring gear fixed to the housing, input on the sun, and output on the planet carrier, according to Equation 2 (Ref. 7).

$$i_0 = -\left|\frac{z_{P1} \cdot z_R}{z_S \cdot z_{P2}}\right| \tag{1}$$

$$i_{SC} = 1 - i_0 = 1 + \left|\frac{z_{P1} \cdot z_R}{z_S \cdot z_{P2}}\right| \tag{2}$$

where
i_0 is the stationary gear ratio [-]
i_{SC} is the gear ratio between the sun gear and carrier [-]
z_S is the number of teeth of the sun gear [-]
z_{P1} is the number of teeth of the first planet [-]
z_{P2} is the number of teeth of the second planet [-]
z_R is the number of teeth of the ring gear [-]

The description of the macrogeometry of cylindrical gear stages requires the specification of certain parameters, which define the geometry without contradiction. Based on these parameters, further macrogeometry parameters can be calculated. Some of the most important values for the geometry calculation of cylindrical gear stages are shown in Figure 2 on the left. For example, the sum of the numbers of teeth Σ_z can be calculated from the center distance a, the helix angle β and the normal module m_n, assuming backlash-free gears without profile shift (Ref. 2). The sum of the numbers of teeth Σ_z is then divided between the two gears, taking the gear ratio i into account. The tip diameter of the first gear is calculated from the tooth root shape of the counter gear and the required tip clearance. In the case of sharp teeth, the tip circle diameter must be reduced so that a minimum tooth thickness is achieved at the tip circle diameter. If the geometry parameters are varied within reasonable limits, the result is a variation space with just geometrically valid gears. The limits of the variation space are not identical for every application. For example, the module m_n should only be increased until the undercut limit is reached on the pinion. Between the minima and maxima, the variation variables lead to valid geometries.

In the design of planetary gear stages, it is necessary to consider characteristics concerning the kinematic couplings. The kinematics of a planetary gear stage is completely determined by one planetary gear. With each additional planetary gear, a kinematic overdetermination takes place, which results in the fact that only special tooth number combinations enable uniform distribution of the planetary gears in the carrier. For simple planetary gear stages, the number of teeth of the sun and the ring gear must fulfill Equation 3. This assembly condition is transferable to stepped planetary gear stages. For a uniform distribution of the planet gears in the carrier, Equation 4 must be fulfilled for stepped planetary gear stages (Ref. 7).

If a variant calculation is carried out for planetary gear stages, an additional variation variable is required for the tool profile of the ring gear, see Figure 2 center. For simple planetary gear stages, due to the double gear mesh on the planetary gear, most of the macrogeometry parameters in both meshes are identical or can be calculated directly. Due to the assembly condition, this calculation also results in nonvalid tooth number combinations, so an iterative calculation is necessary and only a subset of the variation space can be considered further. An additional limitation of the variation space can be made, for example, by the exclusive selection of variants with numbers of teeth without a common divisor.

$$|z_S| + |z_R| = n_P \cdot j \tag{3}$$

$$|z_S \cdot z_{P2}| + |z_{P1} \cdot z_R| = n_P \cdot j \tag{4}$$

where

z_S is the number of teeth of the sun gear [-]
z_R is the number of teeth of the ring gear [-]
z_{P1} is the number of teeth of the first planet [-]
z_{P2} is the number of teeth of the second planet [-]
n_P is the number of (stepped) planets [-]
j is an integer [-]

In the case of stepped planetary gear stages, two geometrically independent gear meshes can be designed and optimized, see Figure 2 on the right. The number of variation variables and thus the number of theoretically available geometry variants is, accordingly, significantly higher. At the same time, the assembly condition according to Equation 4 must be observed, which limits the valid variation space. The numbers of teeth resulting from the gear ratios of the sub-stages must also satisfy the required total gear ratio i_{SC} between sun and carrier, according to Equation 2. Overall, this results in a comparatively large variation space that contains only a few valid geometries. Due to the described restrictions, which can be extended by the exclusive selection of variants with numbers of teeth without a common divisor, an iterative geometry calculation for stepped planetary gears is necessary.

If a comprehensive variation of the parameters of the macrogeometry as well as of the tool profile is performed for all gears, many possible combinations arise. Algorithm-based optimization methods are suitable for selecting a variant within such a large variation space. A full factorial calculation of all geometry variants with high-level calculation methods is not possible in a reasonable calculation time. Nevertheless, with the independent design of the two sub-stages, an increase in power density and efficiency through optimized geometry parameters is conceivable. In the literature, no numerical optimization of the gear geometry of stepped planetary gears is known that combines a tool-based geometry calculation with an FE-based tooth contact analysis.

Objective and Approach

Stepped planetary gear stages can be used to increase the power density in electrically driven vehicles. However, assembly constraints must be considered during design and optimization, which, in combination with a large number of variation variables, require algorithm-based optimization methods. In the design of gearboxes, various design objectives are relevant, which cause conflicts. Therefore, the objective of this paper is the development of a method for algorithm-based design and optimization of the macrogeometry of stepped planetary gear stages, considering weighted design objectives, see Figure 3.

To achieve the overall objective, the boundary conditions in the design of stepped planetary gear stages are first analyzed

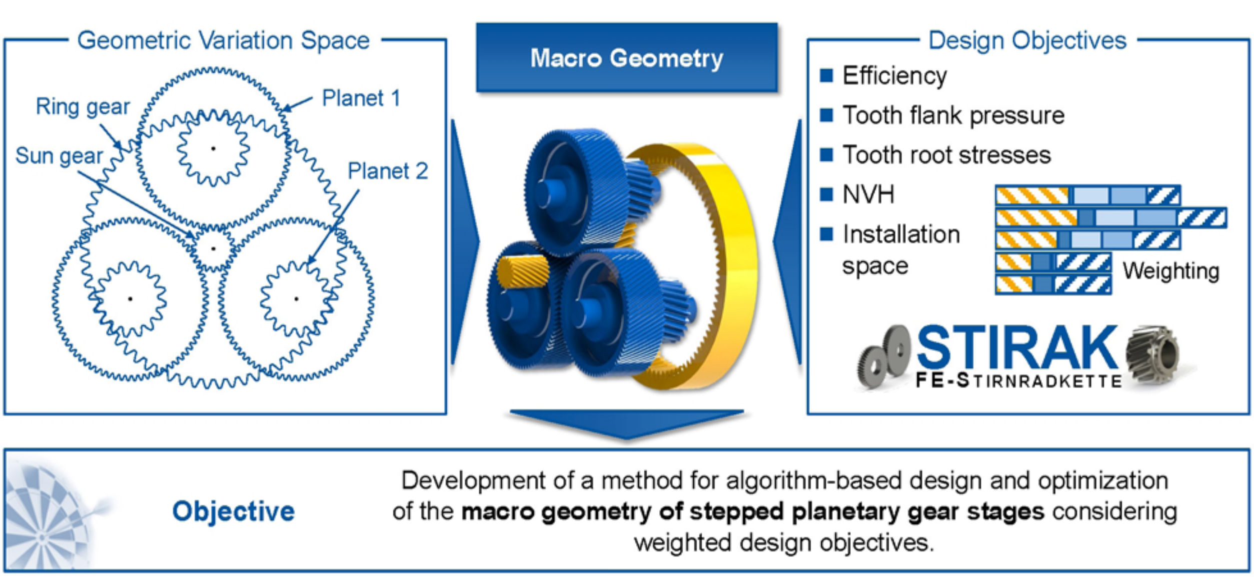

Figure 3 Objective and Approach

in more detail and the geometric variation space is defined. The angular positions of the stepped planets for assembly are derived considering the phase position of the gear meshes. Subsequently, an optimization algorithm is selected that allows an application-oriented evaluation of the gear geometry. The design objectives efficiency, load-carrying capacity, NVH (Noise, Vibration, Harshness), and volume are weighted for different operating points. The operational behavior of the gear geometries is evaluated using the FE-based tooth contact analysis FE-Stirnradkette (Ref. 3). The developed method is then applied to a stepped planetary gear stage of an electrically driven compact car. Different weighting variants of the design objectives are investigated, and the results are compared.

Boundary Conditions for the Design of Stepped Planetary Gear Stages

The assembly constraint of stepped planetary gear stages results from the kinematic coupling of the gear meshes and consequent geometrical restrictions. In this chapter, a method is first presented that enables the identification of suitable tooth number combinations. Subsequently, the phase position of the gear meshes and the necessary assembly angles of the stepped planets are derived. It is assumed that the angle between planet 1 and planet 2 of the same shaft is identical for each of the mounted stepped planets and that they are therefore interchangeable.

Identification of Suitable Numbers of Teeth Combinations

In contrast to simple cylindrical gear stages, the calculation of the numbers of teeth of stepped planetary gear stages is constrained by the mountability. The equation for verifying the mountability was explained in "Design of Stepped Planetary Gear Stages," see Equation 4. Due to the high number of non-mountable geometry variants, a variation of the numbers of teeth with an optimization algorithm is not effective. The number of iterations required to achieve convergence in the optimization can be reduced by avoiding the calculation of non-mountable geometry variants. To exclude these variants, a method for identifying suitable numbers of teeth is presented in the following section. This method uses eight input parameters that lead to one optimal numbers of teeth combination. The eight input parameters can be varied by the optimization algorithm so that only mountable geometry variants are compared during optimization.

The entire procedure for determining the numbers of teeth is shown in Figure 4. The numbers of teeth of the stepped planetary gear stage are determined depending on the eight parameters shown in Figure 4 at the bottom. First, the possible numbers of teeth of the four gears (sun gear, planet 1, planet 2, and ring gear) are varied full factorially in defined ranges. With these, the total gear ratio i_{SC} is calculated in step 2 according to Equation 2. Only variants with a maximum deviation of the total gear ratio of $\Delta i = 0.4$ are selected for further consideration. The number of remaining variants has decreased significantly with this step, see Figure 4.

In the third step, the gear ratio of the first stage (sun-planet 1) of all variants is compared with the target gear ratio of the first stage and used to reduce the number of remaining variants. The permissible deviation of the gear ratio of the first stage is evaluated less restrictively than that of the overall gear ratio since the gear ratio of the first stage is taken up again in step 6. An additional constraint in the identification of the numbers of teeth is the limitation of the greatest common divisor of adjacent gears to $\gcd(z_1;z_2) = 1$, see step 4 in Figure 4. For the remaining variants, the mountability is checked in step 5 according to Equation 4. In addition, a penetration check of the tip diameters of the planet gears is performed, considering the number of stepped planets n_P. The resulting variants contain all tooth number combinations that fulfill the gear ratio requirements and are mountable. In the sixth step, the stepped planetary gear stage is scaled with the center distance a to calculate the normal module m_n of the stages. In the calculation, it is first assumed that the gears are designed without profile shifts and that the center distance a corresponds to the zero center distance ad = a. According to Equation 5, the resulting normal module of each variant $m_{n,var}$ is calculated for both stages. Finally, the variant with a minimum combined deviation according to Equation 6 is selected, see Figure 4, step 6. The deviations from the target values of the normal module of stage 1 $m_{n,1}$, the normal module $m_{n,2}$ of stage

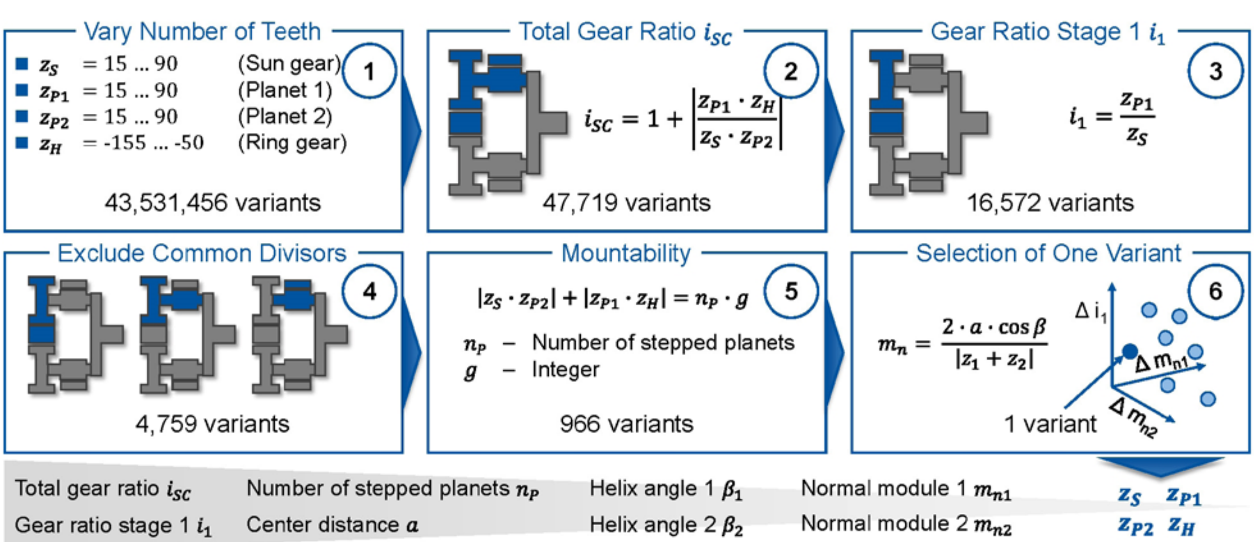

Figure 4 Iterative Identification of Suitable Numbers of Teeth Combinations

2 and the gear ratio of stage 1 i_1 are weighted equally.

$$m_{n,var} = \frac{2 \cdot a_d \cdot \cos\beta}{\Sigma z} \tag{5}$$

$$\min\left(\sqrt{\left(m_{n.1} - \frac{2 \cdot a_d \cdot \cos\beta_1}{z_S \cdot z_{P1}}\right)^2 + \left(m_{n.1} - \frac{2 \cdot a_d \cdot \cos\beta_2}{z_{P1} \cdot z_H}\right)^2 + \left(i_1 - \frac{z_{P1}}{z_S}\right)^2}\right) \tag{6}$$

where

z is the number of teeth [-]

a_d is the zero center distance [mm]

β is the helix angle [°]

m_n is the normal module [mm]

Phase and Assembly Position

Since the mountability of the stepped planetary gear stage is ensured with a suitable numbers of teeth combination, this section considers the necessary positioning of the stepped planets for assembly. As described at the beginning of this chapter, the angle between the two planet gears is assumed to be identical for all stepped planets. In addition, the stepped planets are to be evenly distributed around the circumference of the planet carrier.

A sketch of the gear teeth in assembly position is shown in Figure 5, left. As shown in detail view A, the first tooth gap of the ring gear is in the upper position and is marked with the number 1. The numbering of the tooth gaps on the central gears and the teeth on the planets is in the mathematical positive direction around the z-axis — counterclockwise. The first tooth gap of the sun gear is aligned in the direction of the y-axis. Planet 1 of stepped planet 1 in the sun contact is accordingly aligned with tooth 1 downward in the negative y-direction, see detail view B in Figure 5, right. Planet 2 of stepped planet 1 is oriented upward with tooth 1 in the y-axis direction. With this definition, the positions of the central gears and the stepped planet 1 are fixed. To visualize the rotation angles of the stepped planets, tooth 1 of planet 1 and tooth 1 of planet 2 of each stepped planet are marked with points and are connected with a line.

The calculation of the assembly angle of the second and third stepped planets is derived based on the phase position of the gear meshes of the planet gears and the central gears. First, the phase position of the meshes with the central gears is calculated. The calculation for the sun-planet 1 meshes Δp_{Si} is done according to Equation 7 and correspondingly for the planet 2-ring gear meshes Δp_{Hi} according to Equation 8. The angle $\varphi_{Pin,i}$ describes the angle between the vertical (y-axis) and the connecting line between the centers of the sun and the stepped planet i in the mathematical positive direction. The phase shift in the sun mesh is then converted into a rotation angle of planet 1, see Equation 9. This rotation angle $\varphi_{Pi,\Delta pS}$ ensures that planet 1 is correctly aligned in the sun mesh right, see Figure 5. In the further procedure, the stepped planet i consisting of planet 1 and planet 2 is iteratively rotated by one pitch in the sun-planet 1 mesh, until the phase shift in the planet 2-ring gear mesh corresponds to the previously calculated value Δp_{Hi}. The calculation of the phase shift in the planet 2-ring gear mesh from the rotation of the stepped planet is described in Equation 10. The integer j corresponds to the number of pitches necessary to obtain the required phase shift in the planet 2-ring gear mesh. Finally, the rotation angle for the assembly of the stepped planet i is calculated from the sum of the two angles $\varphi_{Pi,\Delta pS}$ and $\varphi_{Pi,\Delta pH}$, see Equation 11.

$$\Delta p_{Si} = mod\left(\varphi_{Pin,i} \cdot \frac{z_S}{2 \cdot \pi}, 1\right) \tag{7}$$

$$\Delta p_{Ri} = mod\left(\varphi_{Pin,i} \cdot \frac{|z_R|}{2 \cdot \pi}, 1\right) \tag{8}$$

$$\varphi_{Pi,\Delta pS} = \Delta p_{Si} \cdot \frac{2 \cdot \pi}{z_{P1}} \tag{9}$$

$$\Delta p_{Ri} = 1 - mod\left(\frac{\varphi_{Pi,\Delta pS} + j \cdot \frac{2 \cdot \pi}{z_{P1}}}{\frac{2 \cdot \pi}{z_{P2}}}, 1\right) \tag{10}$$

$$\varphi_{Pi} = \varphi_{Pi,\Delta pS} + \varphi_{Pi,\Delta pR} = \varphi_{Pi,\Delta pS} + j \cdot \frac{2 \cdot \pi}{z_{P1}} \tag{11}$$

where

Δp_{Si} is the phase position of the sun-planet 1 meshes [pet]

Δp_{Ri} is the phase position of the planet 2-ring gear meshes [pet]

$\varphi_{Pin,i}$ is the angle of the planet pin position in the carrier [rad]

$\varphi_{Pi,\Delta pS}$ is the rotation angle of the stepped planed due to the phase position in the sun gear mesh [rad]

$\varphi_{Pi,\Delta pR}$ is the rotation angle of the stepped planed due to the phase position in the ring gear mesh [rad]

$z_{S/P1/P2/R}$ is the number of teeth of the sun / planet 1 / planet 2 /

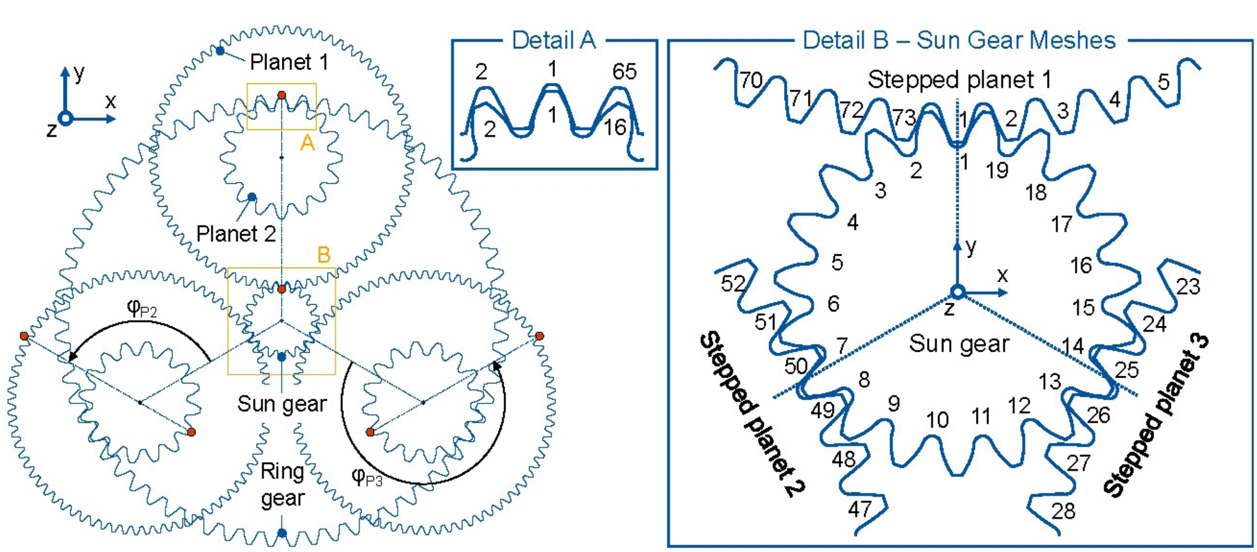

Figure 5 Sketch of the Stepped Planetary Gear Stage in Assembly Position

ring gear [-]
j is an integer [-]
φ_{Pi} is the rotation angle for the assembly of the stepped planet I [rad]

FE-based Macrogeometry Optimization

Numerical optimization methods are used in various engineering areas. In the gearbox design, for example, topology optimization of the housing can be used to reduce the housing mass and increase the stiffness. Optimization of the macro- and microgeometry of the gears is increasingly in focus.

In this paper, a particle-swarm algorithm is used, which is described in more detail in the following section. Then, the constraints, optimization variables, optimization objectives, and their weighting are presented. In contrast to existing optimization methods, an FE-based tooth contact analysis is used to evaluate the operational behavior. Furthermore, a comprehensive variation of different geometry parameters is performed.

Set-up of the Optimization Method

When optimizing the macrogeometry of stepped planetary gear stages, various boundary conditions must be considered. First, a total gear ratio itotal is assumed for the specific application. The number of stepped planets and the microgeometry of the gears are specified as further constraints. For the microgeometry, only a lead crowning and a profile crowning are used. The operating points and evaluation criteria as the last constraints are explained in the next section.

The optimization procedure, the boundary conditions and the optimization parameters are shown in Figure 6. The developed optimization method is based on a particle swarm algorithm with 60 individuals per generation. As can be seen on the right side of Figure 6, the method consists of two processes. First, the particle swarm algorithm creates the input parameters of the next generation. These are computed and evaluated one after the other before the results are provided to the algorithm again and it derives a set of optimized input parameters for the next generation. The total number of generations calculated was chosen as the termination criterion.

When calculating the geometry of the individual variants, the procedure for identifying suitable numbers of teeth is applied as described in the sections before. The geometry parameters that are varied and optimized are listed in Figure 6, bottom left. Since the calculation of the numbers of teeth assumes that the gear teeth are designed without profile shift, the parameter *module deviation* Δm_n is introduced for each gear mesh. With this, the optimization algorithm allows a specific change to the normal module resulting from the calculation of the numbers of teeth. With this change, a sum profile shift becomes necessary at the same time, which is divided between the two gears belonging to one gear mesh with the optimization parameter *profile shift distribution* x_1/x_2. The tool profile for the geometry calculation of the gear teeth is fully rounded at the tip for all calculations. The addendum factor of the tool profile h_{aP0}^* is optimized and thus the tooth root shape is also integrated into the optimization. In total, 18 optimization parameters result, which define the variation space.

The calculation of the characteristic values of each variant is performed with the FE-based tooth contact analysis FE-Stirnradkette. The single gear meshes are calculated independently of each other under quasistatic conditions. Since the shaft-bearing system has not been defined at that stage of design and therefore no load-dependent misalignments can be calculated yet, an ideal alignment of the gear teeth is assumed, see Figure 1. The characteristic values for evaluation and weighting are presented in the following section.

Optimization Objectives and Weighting

In the gear design, the five design objectives load-carrying capacity, excitation behavior, efficiency, cost, and volume can be identified (Ref. 1). With the method presented in this paper, a comprehensive evaluation of all objectives, except cost, is performed. The load-carrying capacity is considered differentiated in terms of maximum tooth flank pressure and maximum tooth root stress. The excitation behavior is evaluated with the peak-to-peak transmission error and the efficiency with the load-related power loss in the gear mesh. The volume is evaluated based on an enveloping cylinder.

The evaluation of the objective values is done with a linear

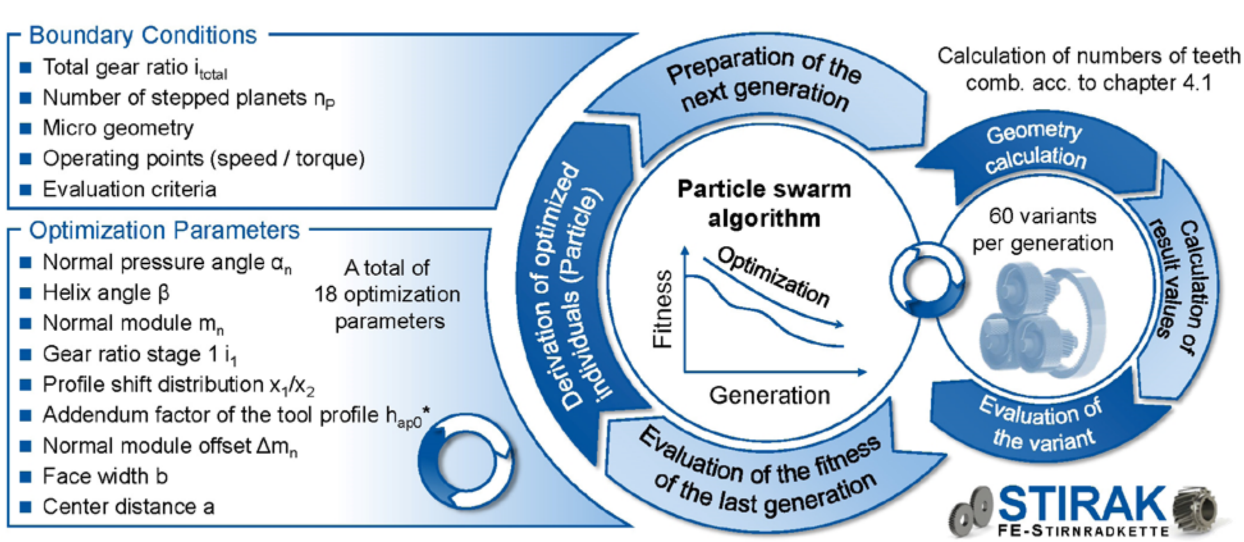

Figure 6 Procedure of the Optimization Method

grade scaling (1–best and 6–worst) for comparability among them. The calculation of the grade *gr* is shown in Equation 12 for a quantity to be minimized for different cases. If the calculated value *v* exceeds the limit value of the grade 6 v_6, an additional deterioration of the grade is applied. This procedure prevents the compensation of different parameters in impermissible ranges.

$$gr = \begin{cases} 1 & v \le v_1 \\ 1 + \frac{5}{v_6 - v_1} \cdot (v - v_1) & v_1 < v \le v_6 \\ 6 + \left(\left(1 + \frac{5}{v_6 - v_1} \cdot (v - v_1)\right) - 6\right) \cdot 5 & v_6 < v \end{cases} \tag{12}$$

where
gr is the grade
v is the value to be graded
v_1 is the value related to grade 1 (best)
v_6 is the value related to grade 6 (worst)

Various operating points consisting of speed and torque are relevant in the gear design. The weighting of the objective values can be different for each operating point. To evaluate a geometry variant, FE-based tooth contact analysis is used to perform calculations at different operating points. Subsequently, the parameters are individually evaluated with grades. The overall evaluation of the geometry variant is calculated according to Equation 13. The procedure for determining the weighting factors of the objective values $w_{k,OP}$ required for the overall evaluation is shown in Figure 7.

$$f = \sum_{op=1}^{n_{op}} \sum_{k=1}^{n_k} w_{k,OP} \cdot gr_{k,OP} \tag{13}$$

where
f is the function value
k is the identifier of the objective value
n_k is the number of objective values
OP is the identifier of the operating point
n_{OP} is the number of operating points
$w_{k,OP}$ is the weighting of the objective value k at the operating point OP
$gr_{k,OP}$ is the grade of the objective value k at the operating point OP

Five relevant operating points were identified for the design, see Figure 7, bottom right. First, the weighting of the design objectives is determined for each operating point, see step 1. The volume of the gear stage is equally relevant for each operating point. In this example, the excitation in the form of the peak-to-peak transmission error is of higher interest in lower torque ranges. In contrast, the characteristic values for the load-carrying capacity are weighted higher at higher torques. In addition to the weighting of the design objectives for each operating point, the weighting of the operating points among each other is also possible. In the example shown, the operating points with higher torque were weighted higher overall, see Figure 7, bottom left. The weighting factors are then normalized so that different weighting variants can be compared, see Figure 7, top right.

Application of the Optimization Method

In this chapter, the developed method for optimizing a stepped planetary gear stage is applied to an electrically driven compact car. First, the use case and the resulting boundary conditions for the optimization are presented. Then, the different weighting variants for the optimization are described and compared. Finally, the optimization results are analyzed and compared with the initial gear design.

Boundary Conditions of the Optimization

The application of the developed method is carried out using the example of an electrically driven compact car. A conventionally driven VW Golf 7 GTI with a maximum output of $P_{max} = 160$ kW was chosen as a reference for comparison. To identify the required boundary conditions of the gearbox, the wheel torque of the conventionally driven vehicle with a 6-speed transmission was plotted against the vehicle speed in Figure 8.

The torque-speed characteristics with six gears of the conventional drivetrain can be approximated with a torque-speed characteristic of an electrical machine. The total power required by the drive unit is divided between two electrical machines, which can be used, for example, as single-wheel drives. The maximum driving speed of the vehicle is limited to $v_{max} = 180$ km/h. With the maximum speed of the electrical machines $n_{EM,max} = 25{,}000$ rpm, the required gear ratio $i_{ges} = 16.60$ is calculated, see step 1 in

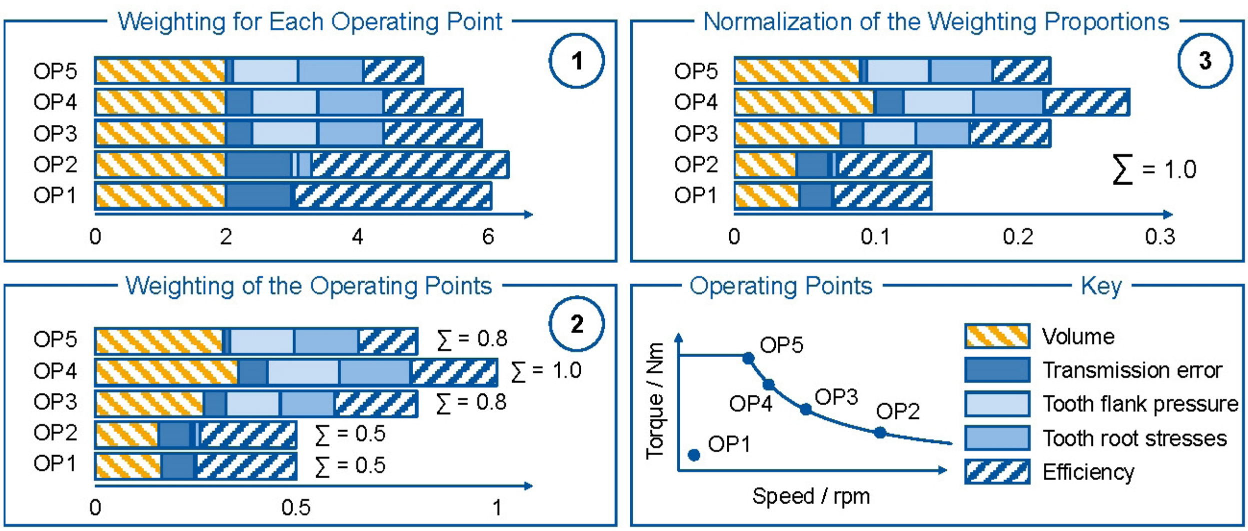

Figure 7 Determination of Weighting Factors for Different Operating Points

Figure 8. A stepped planetary gear stage is therefore suitable for achieving the required total gear ratio. The maximum achievable torque of the electrical machines is then derived from the rated speed of the electrical machine, see step 2 in Figure 8.

Five operating points are identified for the design of the gear stage. The first operating point, OP1, has a low torque and is used during optimization mainly to limit the excitation in the low torque range. The other four operating points are on the maximum power hyperbola and cover a wide torque and speed range.

Description of the Optimization Variants

Ten different weighting variants are selected to optimize the stepped planetary gear stage, see Figure 9. The weighting of the efficiency and the volume is set differently for the variants. The weighting of the remaining optimization objectives — i.e., peak-to-peak transmission error, tooth flank pressure, and tooth root stress — changes accordingly. Starting from variant V11 at the top left in Figure 9, the weighting of the efficiency increases with the variants to the right. The weighting of the volume is increased downwards to variant V14.

A general overview of the variants can be seen in Figure 9, bottom right. The four highlighted weighting variants will be considered in more detail in the next section, as they represent the extrema of the different weightings. In total, three interrelated variant series can be identified. In the variant series V11-V21-V31 and V12-V22-V32-V42-V52, the share of efficiency weighting is progressively increased. The share of volume weighting is progressively increased for the variant series V11-V12-V13-V14. The weighting of the operating points among each other leads to a design focus on the higher torque operating points OP3 to OP5.

Analysis of the Optimization Results

The optimization process of the stepped planetary gear stage was stopped after 100 generations for each weighting variant. A total of 6,000 different geometries were calculated and compared for each weighting variant at five operating points each. For further analysis, the variants were recalculated with a finer resolution of the FE model of the gears. The resulting objective

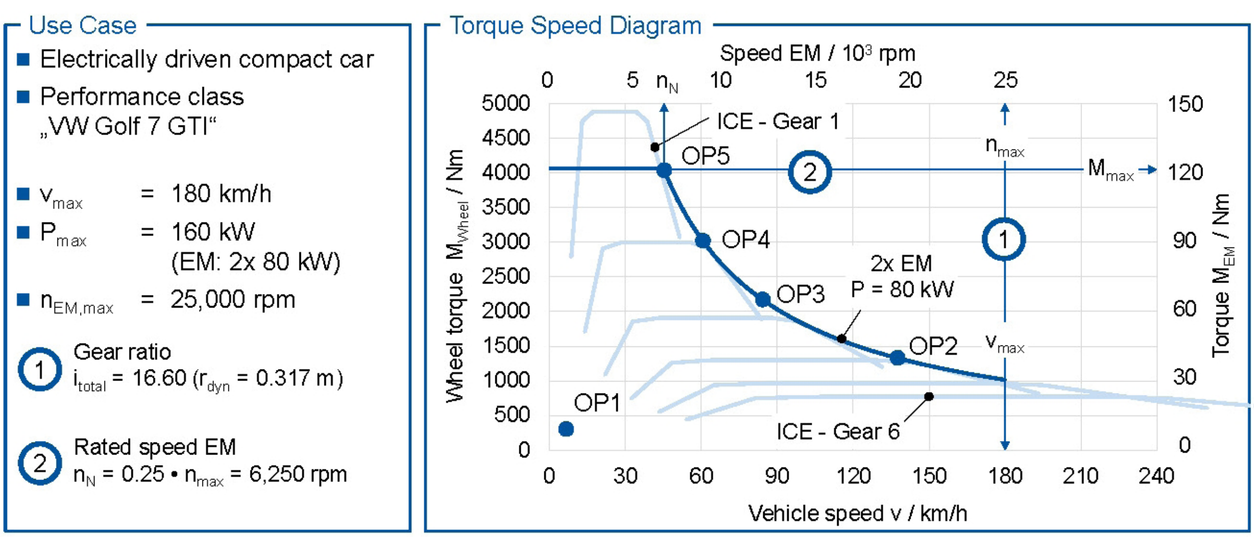

Figure 8 Torque Speed Diagram of the Electrical Machine (EM) and Derivation of Relevant Operating Points (OP)

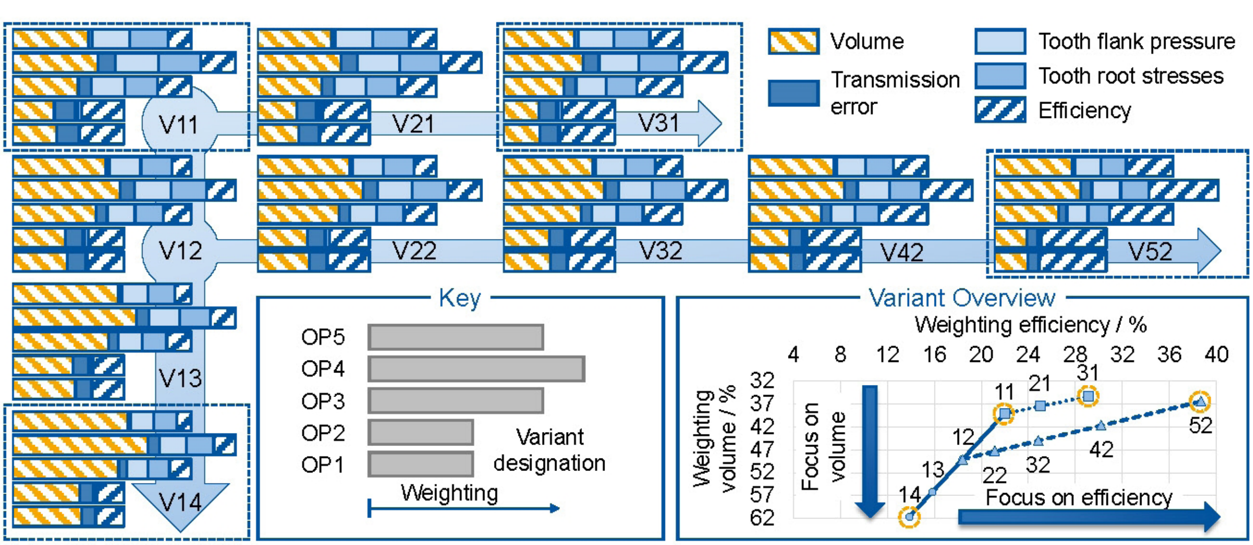

Figure 9 Weighting Variants

values of the optimizations are shown in Figure 10. The theoretical volume of the gear is calculated from the maximum outer diameter and the sum of the face width of the two gear meshes. In Figure 10, top left, the volume of the variants is plotted against the weighting share of the volume. The results show an approximately linear relationship between the weighting and the volume. Variant V14, with the highest weighting of the volume, achieved a 34.3% lower volume than variant V31. The correlations of the different weighting series are recognizable and verify the optimization method.

The results of the second optimization objective, efficiency, are shown in the top right of Figure 10. The diagram shows the mean value of the efficiencies of the two gear meshes for the highest weighted operating point OP4, above the weighting of the efficiency. The increase in the mean efficiency with increasing weighting is visible. The variants converge to a maximum as the weighting increases.

Due to the variation of the two optimization objectives volume and efficiency, the weighting of the other optimization objectives also changes. The results of the other objective values are shown in the same form in Figure 10 below. In particular, the tooth flank pressure and the tooth root stress show a very good correlation between weighting and value.

Four weighting variants were selected for further analysis. The designation and a comparison of the volumes of the different variants can be found in Table 1. With these four variants, the extrema of the weighting series are covered and can be compared with the initial design start. The difference between the variants V31 and V52 is the weighting of the efficiency compared to the weighting of the other optimization objectives. The weighting of the volume is similar so that for variant V31 it can be concluded that the higher volume has a positive influence on the tooth flank pressure and the tooth root stress, see Figure 10 bottom.

Table 1 Theoretical volume of the selected variants

Variant	Main optimization objective	Theoretical volume / l	Rel. change to Start variant
Start		4.385	
V11	Volume / Efficiency	3.866	–11.8%
V14	Volume	2.906	–33.7%
V31	Efficiency (29.1%)	4.427	0.9%
V52	Efficiency (38.7 %)	3.799	–13.4%

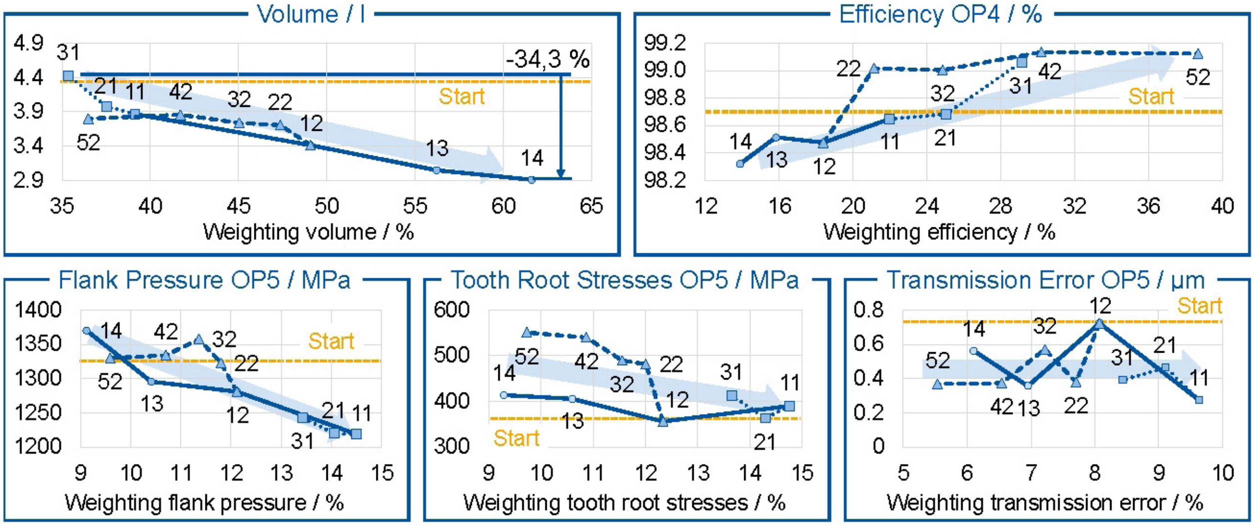

Figure 10 Comparison of the Resulting Key Values of the Different Optimization Variants

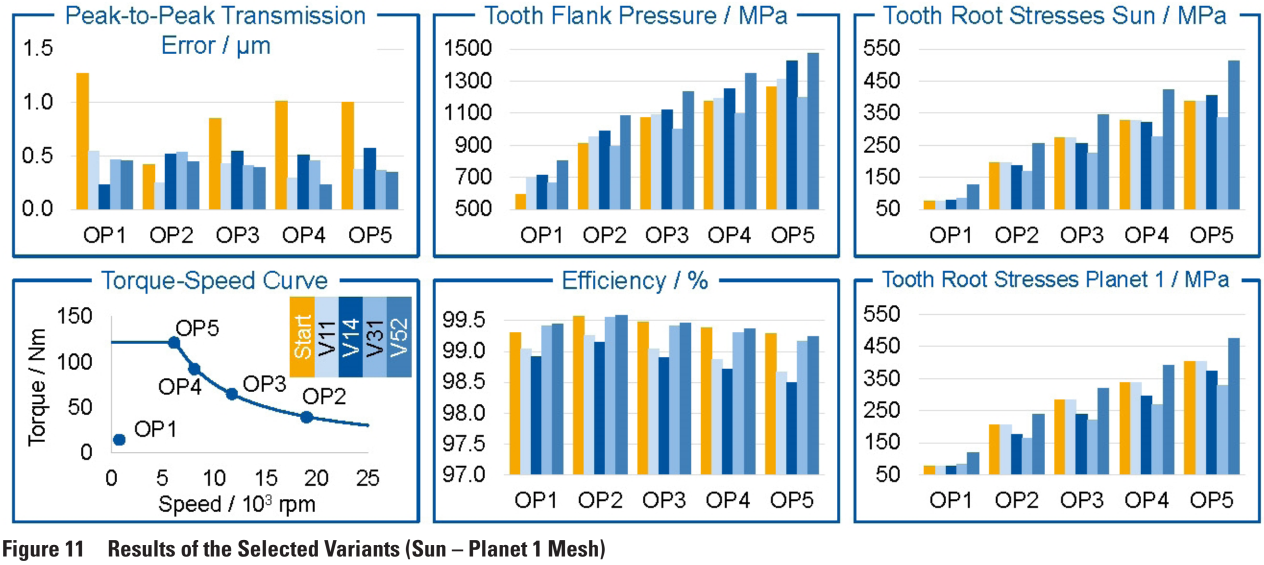

Figure 11 Results of the Selected Variants (Sun – Planet 1 Mesh)

The calculation results of the four selected variants are shown for the sun-planet 1 mesh in Figure 11. First, the significantly lower peak-to-peak transmission error of all optimized variants can be seen. The results for the load-carrying capacity (tooth flank pressure and tooth root stress) of the balanced weighting variant V11 are comparable to those of the variant Start. The volume-optimized variant V14 and the efficiency-optimized variant V52 show a higher tooth flank pressure. On the one hand, this is due to a smaller center distance of both variants and, on the other hand, to a smaller normal module of variant V52. Due to the smaller normal module of variant V52, the tooth root stress of this variant is the highest. The efficiency of variant V31 and variant V52 is comparable to that of variant Start. The assumption that the higher volume of variant V31 compared to variant V52 has a positive influence on the load-carrying capacity with comparable efficiency is shown.

The results for the planet 2-ring gear mesh are shown in Figure 12. The peak-to-peak transmission error is comparable for all variants. The variant Start has the lowest tooth root stress and at the same time the highest tooth flank pressure. The optimized variants offer a more balanced design in terms of load-carrying capacity. The efficiency of the variant Start is the lowest together with the volume-optimized variant V14. The tooth root stress of variant V52 shows the highest value for both gears. The efficiency of variants V31 and V52 is similar and comparatively higher than that of the other variants.

In summary, variant V14, with slightly lower efficiency in the sun-planet 1 mesh, enables a 33.7% reduction in volume. With variant V11, a reduction in excitation is possible with comparable overall efficiency and a simultaneous reduction in volume of 11.8%. The variants V31 and V52 offer increased efficiency and lowered excitation. Depending on the additional dynamic loads and the other boundary conditions of the application, it must be weighted higher for variants V31 and V52 whether the lower volume of variant V52 or the higher load-carrying capacity of variant V31 is more appropriate.

Summary and Outlook

In applications with a high power density and high gear ratio requirements, such as electrically driven vehicles, stepped planetary gear stages can be used. The design of planetary and stepped planetary gear stages is related to assembly restrictions due to their kinematic overdetermination. Generally, numerical optimization methods are increasingly used for gear design. Due to the high number of different design variables for stepped planetary gear stages, optimization methods are suitable for the design and optimization.

The objective of this paper is to develop a method for the algorithm-based design and optimization of the macrogeometry of stepped planetary gear stages. For this purpose, a method for the identification of suitable tooth number combinations is presented first. The developed optimization method offers the advantage of an FE-based evaluation of the operational behavior. A particle swarm algorithm is used to optimize 18 geometry parameters. In the optimization, different operating conditions are considered and weighted against each other.

The developed method is applied to the design and optimization of a stepped planetary gear stage for an electrically driven compact car. For this purpose, ten differently weighted variants are defined and compared. The volume, the efficiency, the peak-to-peak transmission error, the tooth flank pressure, and the tooth root stresses are used as evaluation variables. The weighting components' *efficiency* and *volume* are varied for the different variants.

A comparison of the objective values of the different optimization variants shows a very good correlation between the weighting of an optimization objective and its value. The volume of the gear stage can be reduced by 33.7% for the volume-optimized variant V14. Despite this increase in power density, the characteristic values of the load-carrying capacity of this variant are comparable to those of the initial variant, and the efficiency is only slightly lower. The two other weighting variants analyzed in detail, V31 and V52, offer higher average efficiency than the initial variant.

Overall, the developed method shows further potential in the design and optimization of stepped planetary gear stages. The

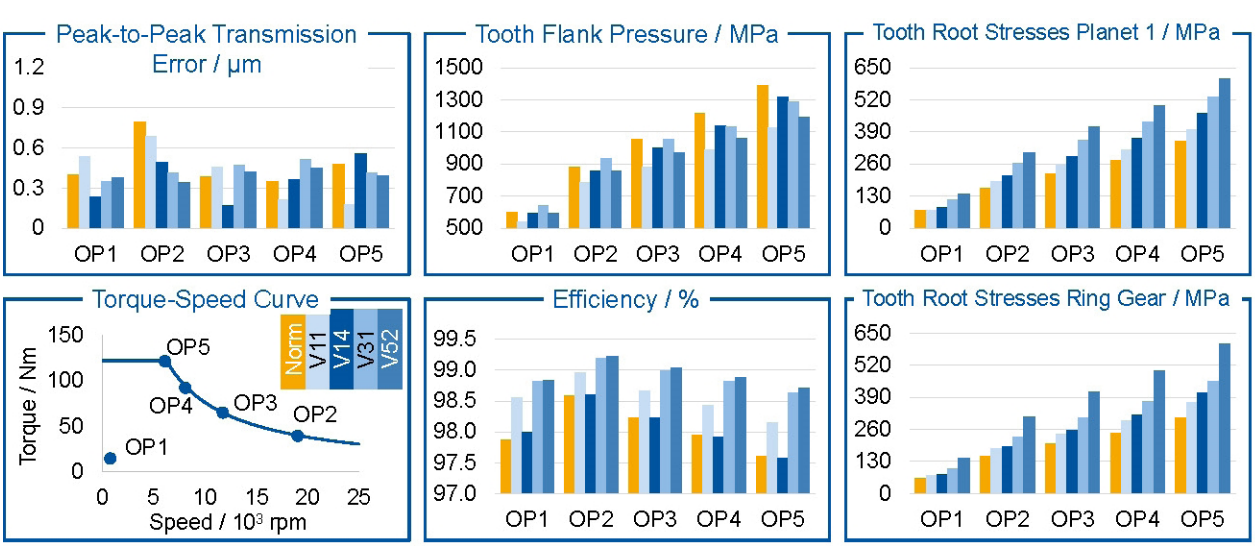

Figure 12 Results of the Selected Variants (Planet 2 – Ring Gear Mesh)

operational behavior of the different optimization variants can be evaluated for a final selection in the multi-body simulation under dynamic operating conditions. Furthermore, an optimization of the microgeometry should be performed, considering the interaction and displacements of the gears.

Bibliography

1. Klocke F.; Brecher C., 2017: Zahnrad- und Getriebetechnik. 1. Aufl, München: Carl Hanser.
2. Norm, 2006: Calculation of load capacity of spur and helical gears. Calculation of surface durability (pitting) (6336 Part 2): Beuth, Berlin.
3. Cao J., 2002: Anforderungs- und fertigungsgerechte Auslegung von Stirnradverzahnungen durch Zahnkontaktanalyse mit Hilfe der FEM. Diss. RWTH Aachen University.
4. Hemmelmann J. E., 2007: Simulation des lastfreien und belasteten Zahneingriffs zur Analyse der Drehübertragung von Zahnradgetrieben. Diss. RWTH Aachen University.
5. Kohn B., 2019: Topologische Flankenkorrektur zur Anregungsoptimierung von Stirnradgetrieben. Diss. TU München.
6. Brimmers J., 2020: Funktionsorientierte Auslegung topologischer Zahnflankenmodifikationen für Beveloidverzahnungen. Diss. RWTH Aachen University.
7. Müller H. W., 1998: Die Umlaufgetriebe. 2. Aufl, Berlin: Springer.

Christian Westphal has been the leader of the Gearbox NVH group at the Laboratory for Machine Tools and Production Engineering (WZL) of RWTH Aachen University since April 2022. His research focuses on the design and the dynamic operational behavior of planetary gearboxes. Westphal graduated from RWTH Aachen University with a master's degree in industrial engineering and management with a major in automotive engineering and corporate development.

Dr.-Ing. Jens Brimmers is the head of the gear department at the Laboratory for Machine Tools and Production Engineering (WZL) of RWTH Aachen University since June 2019. He graduated from RWTH Aachen University with master's degrees in mechanical engineering and business administration. His Ph.D. thesis focused on beveloid gears and topological tooth flank modification.

Prof. Dr.-Ing. Christian Brecher has since January 2004 been Ordinary Professor for Machine Tools at the Laboratory for Machine Tools and Production Engineering (WZL) of the RWTH Aachen, as well as Director of the Department for Production Machines at the Fraunhofer Institute for Production Technology IPT. Upon finishing his academic studies in mechanical engineering, Brecher started his professional career first as a research assistant and later as team leader in the department for machine investigation and evaluation at the WZL. From 1999 to April 2001, he was responsible for the department of machine tools in his capacity as a Senior Engineer. After a short spell as a consultant in the aviation industry, Professor Brecher was appointed in August 2001 as the Director for Development at the DS Technologie Werkzeugmaschinenbau GmbH, Mönchengladbach, where he was responsible for construction and development until December 2003. Brecher has received numerous honors and awards, including the Springorum Commemorative Coin; the Borchers Medal of the RWTH Aachen; the Scholarship Award of the Association of German Tool Manufacturers (Verein Deutscher Werkzeugmaschinenfabriken VDW); and the Otto Kienzle Memorial Coin of the Scientific Society for Production Technology (Wissenschaftliche Gesellschaft für Produktionstechnik WGP).

Siemens

DIGITAL AND SIERRA SPACE COLLABORATE ON DIGITAL ENGINEERING PROGRAM

Siemens Digital Industries Software recently announced that Sierra Space has implemented Siemens' *Xcelerator* software and service portfolio as the foundation for its next-generation digital engineering program. Sierra Space is a commercial space company helping to shape the future of space transportation and infrastructure for the commercialization of Low Earth Orbit (LEO).

The company is implementing *Xcelerator* to create a fully digital environment from development to manufacturing to maintenance. This will help to achieve the goals: Sierra Space wants to develop future solutions for space transport, as well as commercial space travel and infrastructure, and create technologies on which a vibrant, growing and accessible commercial space industry will be built." At Sierra Space, we are building the first platform in space that brings together all aspects of space transportation, space targets and space applications in a holistic ecosystem. It will be a catalyst for the next breakthrough innovations that will also bring many benefits to life on Earth." "Our revolutionary new space platform is being developed using a next-generation digital development environment that we created in collaboration with Siemens," said Tom Vice, CEO of Sierra Space. "Siemens' solutions will significantly accelerate the development of our unique space platform."

Siemens' tools were fundamental to the development of the Dream Chaser. Sierra Space is building on this longstanding collaboration with Siemens to fully transform itself into a digital company. Sierra Space will use Siemens *Xcelerator* at all stages of Dream Chaser's development, including structural, thermal, mechanical, electrical and software design, vehicle manufacturing, requirements review and lifecycle maintenance.

The spacecraft is capable of performing a smooth 1.5g re-entry when transporting crew and cargo and landing on compatible commercial runways worldwide. As a representative of the next generation of space transport, NASA has commissioned the Dream Chaser to carry out cargo delivery and return missions to the International Space Station (ISS). The spacecraft transports up to 5.4 tons per flight. Sierra Space continues to expand this long-standing collaboration with Siemens as the company transforms into a digital enterprise.

In parallel with Dream Chaser, Sierra Space is working to design, develop, build, operate and support a customer-centric goal in Earth orbit. In collaboration with Blue Origin, Sierra Space has developed the Large Integrated Flexible Environment (LIFE)-Habitat, a key component of the Orbital Reef project. This modular, three-story commercial residential and science platform will provide the opportunity for companies from the manufacturing, pharmaceutical and other industries to take advantage of weightlessness. It can be used in low-Earth orbit, on the lunar surface, in lunar orbit and as a transport vehicle to Mars. Sierra Space will use Siemens *Xcelerator* in all phases of LIFE-Habitat development and other space target missions. "We are honored to be working with Sierra Space on their mission to democratize access to space. We look forward to supporting the Sierra Space team in advancing the Dream Chaser product line and LIFE-Habitat with the world's most comprehensive digital twin technology at the heart of their technology strategy," said Tony Hemmelgarn, CEO and chairman, Siemens Digital Industries Software. "This is another in a long list of announcements that show that today's pioneers are using Siemens *Xcelerator* as a platform for real innovation."

sw.siemens.com

Norton Abrasive Process Solutions

OFFERS GRINDING SERVICES

Saint-Gobain Abrasives has introduced its new Norton Abrasive Process Solutions (APS) Program which was established to help customers determine the optimal grinding or finishing solution for the application at hand, ranging from simple to complex, off-hand or automated, and for metal fabrication, production grinding and virtually any abrasives operation. The APS Program draws upon the vast knowledge of the Norton team along with access to 30 different machines, and a new state-of-the-art APS Robotic Automation Cell, which is at the core of the new APS Program located at the Higgins Grinding Technology Center in Northborough, Massachusetts. The APS team provides abrasive process development, optimization, automation and in-house testing. APS services encompass the testing and optimization of new abrasives, improving quality and/ or throughput, and trying entirely new and customized processes.

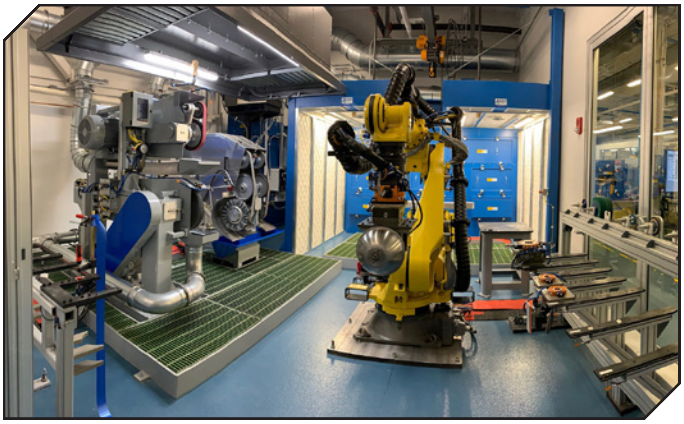

The new APS Program is positioned to be an extension of the customer, where tests can be conducted so that customers do not have to re-assign limited in-house resources and pause their own production. "At a time when North American manufacturers need to deliver high-quality products faster, while stressed with labor shortages, we are thrilled to announce the new APS Program which can relieve some of their burden," said Tony Landes, APS Lead, Norton | Saint-Gobain Abrasives. "The APS Program is uniquely setup to deliver a comprehensive array of services, including a quick response and short turnaround. The APS team can provide the broadest array of grinding and finishing process development solutions for any type of abrasive."

The APS Automation Cell is capable of delivering abrasive-to-part and part-to-abrasive applications, wet/dry processing and uses a full range of abrasives such as coated, non-woven, thin wheel, bonded and superabrasives. Equipped with a verified turnkey solution, manufacturers can then contact an automation system integrator to implement the solution. This avoids costly trial and error at the integrator level.

nortonsga.us/aps

Sandvik Coromant

EXAMINES SUSTAINABLE METALWORKING STANDARDS

As a sustainability advocate and supporter of global sustainability goals, Sandvik Coromant has developed a set of internal goals called Make the Shift to set a new industry standard and raise the bar for sustainable business.

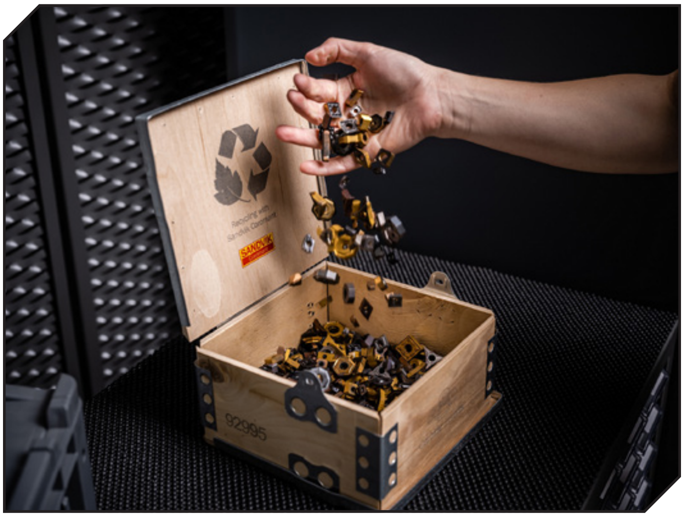

"The metalworking industry is conservative by nature, meaning change can often be slow. We're aiming to disrupt that. We hope that our initiative will motivate other companies in the industry to follow on our path to a more sustainable industry," says Helen Blomqvist, president of Sandvik Coromant.

It's no secret that the industry has a huge carbon footprint. In the US, manufacturing accounts for almost a quarter of direct carbon emissions, according to the Environmental Protection Agency. In Europe, the industry emits an annual total of 880 million tons of carbon dioxide equivalents. Sweeping changes must be made, and Sandvik Coromant is taking major steps to be in the forefront of this transition.

Not only is a more sustainable metalworking industry necessary from environmental aspects, consumers also want companies to be focused on sustainability, as do current and prospective employees. Sandvik Coromant has made a commitment to lead the way toward a more sustainable future — a future where sustainability is the result of what the company does and is an integrated part of how business is conducted. This includes making use of new technologies, new competencies and new ways of designing to make the processes better for both the organization and the environment.

To achieve this, Sandvik Coromant has established two leading objectives:

1. Achieve a more circular business through more efficient recycling, aiming to recycle at least 90 percent of the company's waste and halve the carbon dioxide impact by 2030. Many processes have already been implemented in order to make this shift, from a robust recycling program to digital devices like the Green Factories measurement tool, which allows Sandvik Coromant to track areas of inefficiency throughout all facilities.

2. Increase energy efficiency by repurposing or reducing energy spent in operations, aiming for a 2.5 percent reduction in consumption each year.

As part of Sandvik Coromant's own global recycling process, used carbide tools are collected from customers and sent to the Wolfram Bergbau und Hütten recycling plant, located in Austria. There, recycling managers complete an X-ray fluorescence analysis using a scanning system, which determines the make-up of the received tools. After an initial crushing, the tools form a carbide powder. This powder undergoes chemical purification to retrieve materials that have the same properties as virgin tungsten.

Additional elements in the cemented carbide are also managed sustainably. For example, cobalt retrieved from the tools is sent to a third party for recycling. Carbide tools from all manufacturers are accepted into Sandvik Coromant's recycling program, regardless of size, industry or location.

sandvik.coromant.com/en-us

Eaton

MLOCKER DIFFERENTIAL TURNS 50

Eaton's Vehicle Group is celebrating 50 years of MLocker differential production. The mechanical locking differential provides drivers with best-in-class traction without the need for push-buttons, shift knobs, or other driver intervention, and is applicable to vehicles with both internal combustion engines and electrified vehicles (EVs).

"We're happy to celebrate this important milestone for the MLocker differential, which is built on the success of its predecessor, our popular Posi differential," said Mark Kramer, business unit direct, ePowertrain, Eaton's Vehicle Group. "The unique design and proven quality of the MLocker differential have made it the differential of choice for global full-size pickups and sport-utility vehicles, and even a recently launched electrified urban truck in the Asia-Pacific region."

Utilizing a self-contained, automatic engagement mechanism, the MLocker differential engages in low-traction situations when a wheel speed difference (compared to the other rear wheel) of 100 revolutions per minute (RPM) or greater is detected. Automatic locking takes less than a fraction of a second, improving traction and providing the driver with increased safety and confidence when traveling on wet or icy roads, gravel, mud, and dirt. The MLocker differential is also compatible with existing anti-lock brake and vehicle stability systems, which simplifies OEM integration.

During normal driving conditions, the MLocker differential functions as a light-bias, limited-slip differential. When a low-traction situation occurs that causes a wheel speed difference, a flyweight mechanism opens to engage a latching bracket, triggering a self-energizing clutch system until both axles turn at the same speed (full lock), thereby preventing further wheel slip. Unlocking occurs automatically and the differential resumes normal operation.

The MLocker differential has undergone modifications over its long production run, but the foundational design and concept have remained constant.

"Functionally it's the same design, but we have made a lot of improvements over the years. Our initial concept has weathered the test of time, although it's been consistently improved to meet the needs of the industry," said Keith E. Morgensai, an engineering specialist who has been involved in MLocker differential engineering and evolution for more than 40 years.

"It's deceptively simple, but there is an awful lot of engineering that went into its development," Morgensai said.

Since launching the MLocker differential, Eaton's Vehicle Group has continued to add to its differentials portfolio that offers solutions for all user profiles.

eaton.com

AGMA

ANNOUNCES NEW BOARD OF DIRECTORS

The American Gear Manufacturers Association (AGMA) announced the changing of its board of directors at the 2022 AGMA Annual Meeting held March 31 through April 2 in Palm Beach Gardens, Florida.

American Gear Manufacturers Association

The four outgoing members served from 2019–2022 include Zen Cichon, president, Avers Machine and Gear (Innovative Rack and Gear), Ruthie Johnston, president and CEO, Croix Gear and Machining, Scott Miller, gear engineering technical steward, Caterpillar and Sara Zimmerman, vice president, business development, Sumitomo Drive Technologies.

Additionally, AGMA welcomes four new members serving a three-year term from 2022–2025. The new members were elected by AGMA corporate members in the first quarter of 2022 and announced during the 2022 AGMA Annual Meeting.

The newly elected board members include Joe Goral, director of sales and marketing, Bourn & Koch, Inc., Michelle Maddox, sales and business development manager, B&R Machine and Gear Corp., Nicole M. Wolter, president and CEO, HM Manufacturing and Scott Yoders, vice president, sales, Liebherr Gear Technology, Inc.

"AGMA is very lucky to have a continuous group of members that come to join the board of directors to further the power transmission industry," stated Matthew E. Croson, president, AGMA. "I look forward to working with our incoming board and thank all of those leaving for their service."

agma.org

MachineMetrics

OFFERS EBOOK ON MACHINE CONNECTIVITY

Most manufacturers are unable to capture and analyze the thousands of data points produced by modern manufacturing equipment because, until recently, it has been far too difficult to do so.

This lack of data often leads to massive inefficiencies that affect every component of a company's operations, including an inability to drive process improvements, justify capital expenditures, and identify unexpected machine failures.

MachineMetrics has released a new eBook, *A Manufacturer's Guide to Machine Connectivity* to examine the challenges manufacturers face when attempting to connect OT assets, the main components involved with machine connectivity, (manufacturing equipment, industrial protocols, IoT hardware, and data standardization) and how to select a solution that offers simple, scalable, interoperable connectivity and autonomous data collection and standardization. Download the book here:

machinemetrics.com

GF Machining Solutions

INVESTS IN NORTH AMERICAN MEDICAL MANUFACTURING

Underscoring its commitment to the support of advanced medical manufacturing, GF Machining Solutions has established a Medical Center of Competency and has appointed a new Medical Business Development Manager, **Donn Wuestenberg,** to head its operations. The new center, scheduled to open later this year in Lincolnshire, Ill., will provide medical manufacturers in North America with comprehensive applications support along with world-class production technologies that include precision milling, EDM, laser texturing, micromachining and automation.

At the center, manufacturers will have access to the GF Machining Solutions sales and service as well as industry leading medical application support teams. With extensive experience in the manufacture of complex, high-precision parts, the company will provide strategies and technologies for improving the production of medical instruments, orthopedic and trauma implants, consumables, dental parts, packaging and more.

According to Wuestenberg, the new Medical Center of Competency will provide the perfect environment for collaboration between GF Machining Solutions, its medical customers and key industry partners. "Together," he said, "we can identify and focus our efforts on those transformational projects that will further advance the medical manufacturing industry sector. These collaborations will also help spur the development of new and refined machines and technologies that will keep North American medical manufacturers moving forward and competitive."

Wuestenberg brings more than 20 years of manufacturing experience with a strong focus on working collaboratively with key technology partners to his new position at the center. He is a Master Electrician and Journeyman Industrial Electrician and possesses extensive expertise in plant production, project design, die/mold and production machinery for medical parts.

gfms.com

MPIF

ANNOUNCES LATEST EDITION OF PM STANDARD METHODS

The 2022 Edition of *Standard Test Methods for Metal Powders and Powder Metallurgy Products* is now available for purchase. The most current versions of these standards, which are used in the manufacture of both metal powder and powder metallurgy products, are required by quality assurance programs to maintain full compliance.

This new volume contains 48 standards covering terminology and recommended methods of test for metal powders, powder metal and metal injection molded parts, metallic filters, and powder metallurgy equipment, and metal additive manufacturing (AM).

The 2022 edition includes three new standards on preparing and evaluating tension test specimens for metal AM and flow rate of metal powders using the Carney flowmeter funnel.

Additionally, an updated version of *A Collection of Powder Characterization Standards for Metal Additive Manufacturing* is available containing 12 existing MPIF Standard Test Methods that can be applicable for the characterization of powders used in metal AM processes.

mpif.org

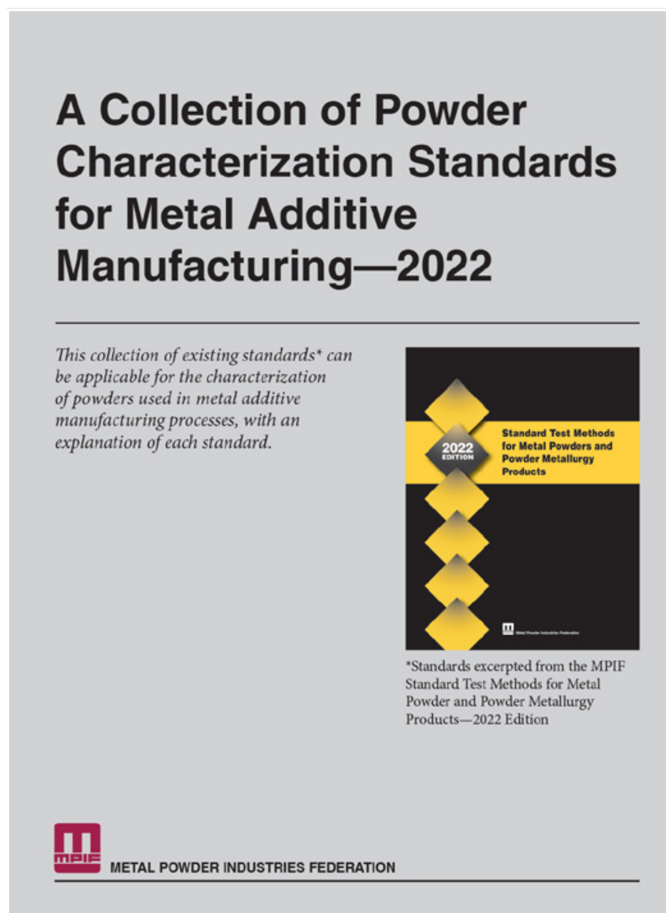

June 7–9 — Eurotrans Gear Weeks 2022

Eurotrans Gear Training will be held online with live online presentations by top industry experts - three weeks packed with specialized gear design training. This comprehensive online course has been developed by Eurotrans, the European Committee for Power Transmission Engineering, in cooperation with FVA Software & Service, and leading gear experts from Germany. This course is oriented to people active in the gears sector with a basic engineering background and provides improvement of knowledge on geometry and design aspects of gears and gear systems. Further, this course is given in English and contributes to improve the language skills of the participants by interacting with the experts and with their peers from other countries.

fva-service.de

June 21–24 — Automatica 2022

Automatica (Munich) is a trade fair for smart automation and robotics. The show brings together all key technologies in the international technology hub of Munich for an exchange between industrial, research and political representatives. It offers an overview of global developments, topics, innovations, and solutions from automated to autonomous production. Exhibitors include Liebherr, Nidec, Moog, Bosch Rexroth, Schaeffler, Festo, Igus and more.

automatica-munich.com/en

July 19–21 — AGMA Gearbox Systems Design

This course (Clearwater Beach, Fla.) focuses the supporting elements of a gearbox that allow gears and bearings to do their jobs most efficiently. Learn about seals, lubrication, lubricants, housings, breathers, and other details that go into designing gearbox systems. Gear design engineers; management involved with the design and manufacture of gearing type components; metallurgists and materials engineers; laboratory technicians; quality assurance technicians; furnace design engineers; and equipment suppliers should attend. The course is instructed by Ray Drago and Steve Cymbala.

agma.org/education/advanced-courses/2022-gearbox-systems-design

July 25–28 — Reliable Plant 2022

This three-day event (Orlando, Fla.) offers attendees learning sessions and case studies on the latest industrial lubrication and oil analysis technologies. The comprehensive conference schedule covers every facet of the machinery lubrication industry and includes workshops on topics such as employee performance, lubrication fundamentals, condition-based maintenance and maintenance planning. Reliable Plant is focused on both entry level and management positions within the lubrication industry including engineers, plant managers, maintenance professionals, safety personnel, planners, quality managers and more.

conference.reliableplant.com

July 26–28 — AGMA Heat Treat Operator/ Operations

This course provides the heat treat operator and operations team, the means to perform the heat treatment of steel gears in a manner that meets the AGMA and customer requirements in a safe and efficient manner. The course identifies the key requirements for proper processing. Sufficient metallurgical background is provided to allow the student to identify how this information relates to the required processing and properties of the gear. This course is taught at the AGMA National Training Center at Daley College, Chicago, Ill., by Carl Ribaudo.

agma.org/education/advanced-courses/2022-gear-heat-treatment-operator-operations

ad index

gear TECHNOLOGY

FREE SUBSCRIPTION

18GTPAGE

RESPONSE REQUIRED

☐ **YES** I want to receive/continue to receive ***Gear Technology***

☐ **NO** Thanks anyway, but I don't need the world's best publication on gear engineering and manufacturing.

Name ______________________ Job Title ______________________
(please print)

Signature ______________________ Date ______________________
(required)

How would you like to receive *Gear Technology*?

- ☐ PRINT version (Verify mailing info below)
- ☐ DIGITAL Version (E-mail required)
- ☐ BOTH Print AND Digital (E-mail required)

E-mail ______________________*

***Your PRIVACY is important to us. You get to CHOOSE how we use your personal information. The next e-mail we send you will have clear instructions.**

How are you involved with GEARS?

- ☐ My company MAKES GEARS (20)
- ☐ My company BUYS GEARS (22)
- ☐ I DESIGN gears (23)
- ☐ I am a SUPPLIER to the GEAR INDUSTRY (24)
- ☐ OTHER (Please describe) ______________________

What is your company's principal product or service? ______________________

____

MAILING INFORMATION

NAME:

JOB TITLE:

COMPANY:

ADDRESS:

☐ Check if this is a home address

CITY:

STATE/Province:

ZIP/Postal Code:

PHONE:

FAX:

Put your business card here to make it easier!

Mail to:
1840 Jarvis Ave., Elk Grove Village, IL 60007 USA

or

FAX to 1-847-437-6618
SCAN to: subscribe@geartechnology.com

Ear-to-Gear Ratio: An Uncanny Valley of Sound

What will the future sounds of vehicles be?

Aaron Fagan, Senior Editor

When it comes to noise, vibration and harshness (NVH), I'm reminded of that dog-van scene from *Dumb and Dumber* where Jim Carrey says, "Want to hear the most annoying sound in the world?" and then proceeds to emit an astonishingly awful noise. Annoying as NVH may be, it's a key metric in drive-system development for e-mobility, and the careful design and manufacture of gears are crucial to minimizing NVH as tolerance variations can result in large differences between nominally identical components. Failure to factor for NVH will force manufacturers to adopt absorbent masking techniques that will add weight or cost or both — plus reduce energy efficiency. And the exterior sound is tightly regulated in most road vehicles, but while internal combustion engine (ICE) cars must be quieted, governments require almost silent EVs and hybrids to be equipped with acoustic vehicle alerting systems to improve safety for pedestrians. This presents a challenge as well as an opportunity to automakers to design sounds that conform to these regulations but that also project the correct character for the vehicle and the brand. So, vehicles will sound like *something,* but what will that be?

In 1970, a Japanese professor of robotics, Masahiro Mori, identified a phenomenon he referred to as *bukimi no tani genshō,* which was subsequently translated into English as the "uncanny valley" by Jasia Reichardt in her 1978 book *Robots: Fact, Fiction, and Prediction*. The uncanny valley is meant to describe the extent to which something synthetic resembles something familiar — and the intuitive distance we perceive, between what's real and unreal, conjures a negative emotional response, a sense of unease as if we know we are in the presence of something false. Research has been conducted on the uncanny valley in various contexts, including sound.

Psychoacoustics — the science of the relationships between aural stimuli and the responses NVH produces in people — isn't the branch of engineering that leaps to mind when considering all the disciplines required for developing vehicles. While *noise* and *vibration* cede to objective measurement, *harshness* involves a more subjective assessment. The soundscape in and around an EV is culturally unfamiliar, so it will be subject to intensive R&D effort as OEMs strive to make their vehicles and brands more distinctive.

What would be considered normal road noise and vibration in an ICE may seem harsher or rougher in an EV because of the way we perceive and process sound and vibration. Vehicle gearbox whine is a common NVH problem that causes troubling quality and performance issues, but to fix the phenomenon efficiently and fundamentally, something must be done to control the ambient air that is the main transfer path of radiation noise. Because the frequencies correspond with the upper end of human hearing, these sounds can be painful.

It's important to analyze the components, systems, and assemblies that make up a complete vehicle both separately and together. The overall soundscape is the whole of acoustic sources and takes into account the transfer path of each one to the driver's and passengers' ears.

Improved acoustic comfort can come at the cost of increased weight which affects the vehicle's overall energy efficiency. However, the growing pressure for energy efficiency presents NVH engineers with a continuously shrinking weight budget. Ideally, future structural design and optimal integration strategies will minimize transfer paths because noise-dampening materials should be a last resort.

It also bears mentioning that, at some point, sound engineers will be faced with a host of new expectations for the interior experience of autonomous shared vehicles from riders rather than drivers and customers rather than owners. Because driving will no longer be the focus of attention in a self-driving car. And personalization will take other forms when: "You'll own nothing. And you'll be happy. Whatever you want, you'll rent. And it will be delivered by drone." In 2016, that was number one of eight predictions The World Economic Forum submitted for what the world will look like in 2030.

Apart from what Hollywood's sound engineers have done to bring the vehicles of science fiction to life in film, there isn't a common precedent for what an EV should sound like to us. There are many psychoacoustic roads that can be taken toward that end, which could involve altering the real sounds of an EV into something as familiar as an ICE (not unlike the principle of an ICE vehicle being equipped with a sound symposer to make it sound more like, ironically enough, an ICE) or something entirely novel that manufacturers may develop into their signature sound for the electrification era.

Whatever direction we venture into the uncanny valley of sci-fi vehicle sound design, the biggest takeaway is that — while synthesized sources have a place — there is a special part of our consciousness that more readily finds the most compelling sounds originate from organic sources like the laugh tracks that were meant to simulate a live studio audience on television.